



## Seasonal carbon dynamics of the Kolyma River tributaries, Siberia

Kirsi H. Keskitalo<sup>1,2\*</sup>, Lisa Bröder<sup>1,3</sup>, Tommaso Tesi<sup>4</sup>, Paul J. Mann<sup>2</sup>, Dirk J. Jong<sup>1</sup>, Sergio Bulte Garcia<sup>1</sup>, Anna Davydova<sup>5</sup>, Sergei Davydov<sup>5</sup>, Nikita Zimov<sup>5</sup>, Negar Haghypour<sup>3,6</sup>, Timothy I. Eglinton<sup>3</sup> and Jorien E. Vonk<sup>1\*</sup>

5 <sup>1</sup>Department of Earth Sciences, Vrije Universiteit Amsterdam, Amsterdam, The Netherlands

<sup>2</sup>Department of Geography and Environmental Sciences, Northumbria University, Newcastle Upon Tyne, UK

<sup>3</sup>Department of Earth Sciences, Swiss Federal Institute of Technology, Zürich, Switzerland

<sup>4</sup>National Research Council, Institute of Polar Sciences in Bologna, Italy

10 <sup>5</sup>Pacific Geographical Institute, Far East Branch, Russian Academy of Sciences, Northeast Science Station, Cherskiy, Republic of Sakha, Yakutia, Russia

<sup>6</sup>Laboratory of Ion Beam Physics, Swiss Federal Institute of Technology, Zürich, Switzerland

*Correspondence to:* Kirsi H. Keskitalo (kirsi.keskitalo@northumbria.ac.uk) and Jorien E. Vonk (j.e.vonk@vu.nl)

**Abstract.** Arctic warming is causing permafrost thaw and release of organic carbon (OC) to fluvial systems. Permafrost-derived OC can be transported downstream and degraded into greenhouse gases that may enhance climate warming. 15 Susceptibility of OC to decomposition depends largely upon its source and composition which varies throughout the seasonally distinct hydrograph. Most studies to date have focused on larger Arctic rivers, yet little is known about carbon dynamics in lower order rivers/streams. Here, we characterize composition and sources of OC, focusing on less studied particulate OC (POC), in smaller waterways within the Kolyma River watershed. Additionally, we examine how watershed characteristics control carbon concentrations. In lower order systems, we find rapid initiation of primary production in response to warm 20 weather, shown by decreasing  $\delta^{13}\text{C}$ -POC, in contrast to larger rivers. As Arctic warming and hydrologic changes may increase OC transfer from smaller waterways through river networks this may intensify inland water carbon outgassing.

### 1 Introduction

The Arctic is warming up to four times the rate of the global average (Meredith et al., 2019; Rantanen et al., 2022) which affects hydrology, carbon cycling and permafrost (Turetsky et al., 2019; Walvoord and Kurylyk, 2016). Terrestrial permafrost 25 thaw adds organic carbon (OC) to fluvial systems via active layer leaching and abrupt thaw processes (e.g., river bank erosion), the former releasing predominantly dissolved OC (DOC) and the latter particulate OC (POC) (Guo et al., 2007; Schuur et al., 2015). Mineralization of terrestrially derived permafrost OC in fluvial systems adds greenhouse gases into the atmosphere enhancing climate warming (Meredith et al., 2019; Schuur et al., 2015).

30 Mineralization dynamics of fluvial OC are largely determined by its composition. Modern-aged DOC predominantly fuels  $\text{CO}_2$  emissions from Arctic waters (Dean et al., 2020), yet permafrost DOC is preferentially degraded when present (Mann et al., 2015; Vonk et al., 2013). The fluxes, composition, and degradation of mainstem-POC have been addressed in large Arctic



rivers (e.g., Bröder et al., 2020; Guo and Macdonald, 2006; Keskitalo et al., 2022; McClelland et al., 2016), but our understanding of the carbon dynamics, especially regarding POC, and seasonality of smaller waterways are lacking.

Here, we investigate carbon characteristics (POC, DOC, dissolved inorganic carbon - DIC, stable carbon isotope  $\delta^{13}\text{C}$  of these carbon pools, and radiocarbon  $\Delta^{14}\text{C}$ -POC) and water chemistry (temperature, pH, conductivity, and water isotopes  $\delta^{18}\text{O}$  and  $\delta^2\text{H}$ ) in lower order streams/ivers within the Kolyma watershed (Fig. 1). We perform source-apportionment modelling to characterize sources of POC, and investigate how seasons and spatial characteristics (e.g., slope, soil OC content) affect carbon contributions in these streams. A future intensification of the Arctic hydrological cycle combined with longer growing season, earlier onset of spring freshet and on-going permafrost thaw is expected to shunt organic matter more rapidly from land into lower order streams/ivers and into large river systems. It is therefore necessary to understand carbon dynamics of lower order systems in order to project future changes within Arctic rivers (Collins et al., 2021; Mann et al., 2022; Raymond et al., 2016; Stadnyk et al., 2021).

## 2 Materials and Methods

### 2.1 Study area and background

The Kolyma River drains 100 % continuous permafrost terrain (Holmes et al., 2012) with variable landscapes including wetlands, tundra and forests (Mann et al., 2012). Here, permafrost consists partially of the OC- and ice-rich Yedoma sediments, which date to the Pleistocene (Strauss et al., 2017, 2021; Zimov et al., 2006). The continental climate encompasses cold winters (January mean  $-32.7\text{ }^\circ\text{C}$ ) and mild summers (July mean  $13.2\text{ }^\circ\text{C}$ ) (Fedorov-Davydov et al., 2018b). River hydrology is characterized by a discharge peak ( $>30,000\text{ m}^3\text{ s}^{-1}$ ) during spring freshet (May–June), followed by a lower discharge (average of  $6,200 \pm 3000\text{ m}^3\text{ s}^{-1}$  in 2007–2017) during summer (July–August) (Shiklomanov et al., 2021). River OC concentrations follow the same pattern as discharge with higher concentrations during freshet than summer (Holmes et al., 2012; McClelland et al., 2016). All tributaries investigated in this study are partially underlain by Yedoma and located within the taiga or the tundra zone (Fig. 1) (Siewert et al., 2015; Strauss et al., 2021, 2022). Mean active layer thickness varies between catchments ranging from 154 cm in Panteleikha, 90 cm across the uplands (Y3), 65 cm at Ambolikha and 48 cm in tundra (measured at Cape Maliy Chukochiy) (Fedorov-Davydov et al., 2018a, 2018b).

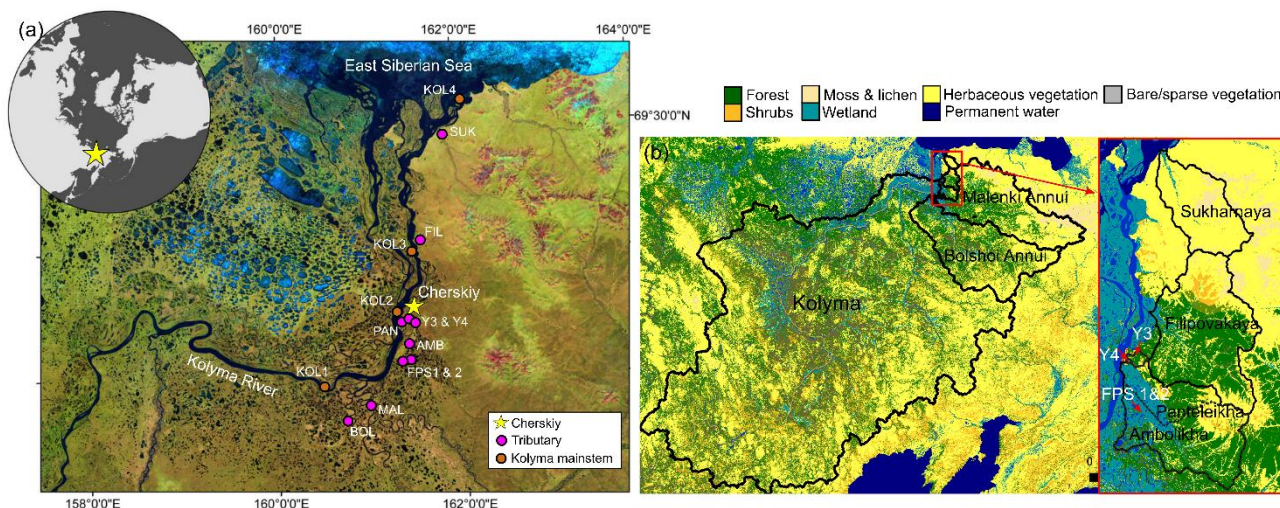


**Figure 1.** (a) Sampling locations of the Kolyma River and tributaries (i.e., lower order streams). The tributaries are Sukhar'naya (SUK), Filipovkaya (FIL), Panteleikha (PAN), Malenki Annui (MAL) and Bolshoi Annui (BOL). Ambolikha (AMB), Y3 and Y4 are tributaries of Panteleikha, and floodplain streams (FPS1 and FPS2) tributaries of Ambolikha. All the sites were sampled in both seasons: summer (July–August 2018) and freshet (June 2019). Map adapted from Mann et al. (2012) (b) Land cover of the Kolyma and its tributary watersheds. Land cover classes according to Buchhorn et al. (2020).

## 2.2 Field sampling

Surface water samples were collected in summer (July–August) 2018 and spring (June) 2019 (Fig. 1, Table A1) from ~20 cm depth from the middle of the tributary river/stream (one sample per river/stream per season, total n=10 tributaries per season) and additionally in the Kolyma mainstem (n=6 in spring and n=4 in summer) using pre-rinsed 1 L Nalgene bottles, which were decanted into a 10 L sterile and pre-rinsed polyethylene bag to maximize the sample size. Water quality parameters were recorded using a multi-parameter sonde (Eijkelpamp Aquaread AP-800 in 2018, YSI Professional Plus in 2019).

Water samples were filtered (within 12 h) using pre-combusted (350 °C, 6 h) glass-fiber filters (Whatman, 0.7 μm). Prior to filtering, samples were vigorously agitated to ensure thorough particle mixing. Filters (POC samples) were frozen to -20 °C, while the filtrate (DOC samples, ~30 ml) was acidified with 30 μl of HCl (37 %) and stored cool (+5 °C). Samples for stable water isotopes ( $\delta^{18}\text{O}$ ,  $\delta^2\text{H}$ ) were filtered and stored cool (+5 °C) without headspace.

## 2.3 Analytical methods

### 2.3.1 Total suspended solids, organic carbon, and carbon isotope analyses

The amount of total suspended solids (TSS, mg L<sup>-1</sup>) was calculated by the difference in filter weight before and after filtering, divided by the volume of water filtered. For POC concentrations,  $\delta^{13}\text{C}$ -POC and total particulate nitrogen (TPN) filters were freeze-dried and subsampled by punching 18 % of the 45 mm filter area and fitted into silver capsules/boats. The subsamples were treated with 1M HCl to remove inorganic carbon, and then placed into an oven at 60 °C until dry. Afterwards, the samples



were wrapped in tin capsules/boats to aid combustion during analysis. The samples were analyzed with a Thermo Fisher Elemental Analyzer (FLASH 2000 CHNS/O) coupled with a Thermo Finnigan Delta plus isotope ratio mass spectrometer (IRMS) at the National Research Council, Institute of Polar Sciences in Bologna, Italy.

For the  $^{14}\text{C}$  analysis, filters (see above for the subsampling method) were fumigated over 37 % HCl (72 h at 60 °C) to remove all inorganic carbon. After fumigation, samples were neutralized of excess acid (60 °C, a minimum of 48 h) in the presence of NaOH pellets, and subsequently wrapped in tin boats. The samples were analyzed using a coupled elemental analyzer-accelerator mass spectrometer (EA-AMS) system (vario MICRO cube, Elementar; Mini Carbon Dating System MICADAS, Ionplus, Dietikon, Switzerland) (Synal et al., 2007). The filter samples were blank corrected for constant contamination according to the method presented in Haghypour et al. (2019). The  $^{14}\text{C}$  analysis was carried out at the Laboratory of Ion Beam Physics at the Swiss Federal Institute of Technology (ETH), Zürich, Switzerland.

The DOC samples from summer 2018 were analyzed for OC and  $\delta^{13}\text{C}$ -DOC with an Aurora 1030 TOC analyzer (OI Analytical) coupled to a Delta V Advantage IRMS via a custom-built cryotrapping interface at KU Leuven, Belgium. Quantification and calibration were performed with IAEA-C6 ( $\delta^{13}\text{C} = -10.4 \text{ ‰}$ ) and an in-house sucrose standard ( $\delta^{13}\text{C} = -26.9 \text{ ‰}$ ) prepared in different concentrations. All  $\delta^{13}\text{C}$  data are reported in the notation relative to VPDB (Vienna Pee Dee Belemnite). The precision in duplicate samples was <5 % for DOC, and 0.2 ‰ for  $\delta^{13}\text{C}$ -DOC in >95 % cases. The DOC samples from freshet 2019 were analyzed for OC and  $\delta^{13}\text{C}$ -DOC at the North Carolina State University, Raleigh, USA. For the method details, see Osburn and St-Jean (2007).

### 2.3.2 Dissolved inorganic carbon analyses

Samples for DIC were collected by filtering 4 ml of water into pre-evacuated 12 ml exetainer (Labco, UK) containing 100  $\mu\text{l}$  of  $\text{H}_3\text{PO}_4$  in 2018, while in 2019, DIC samples were filtered into exetainers containing 100  $\mu\text{L}$  of saturated KI and filled to the rim. The samples were stored cool (+5 °C) and dark until analysis. Headspace  $\text{CO}_2$  of the DIC samples from 2018 was analyzed using a Gasbench interfaced to a Thermo Delta V IRMS at the Northumbria University, UK. The DIC samples from 2019 were inserted into exetainers (pre-flushed with He) containing three drops of concentrated  $\text{H}_3\text{PO}_4$ . Subsequently, the  $\text{CO}_2$  was measured with a Finnigan GasBench II interfaced with a Thermo Finnigan Delta+ mass spectrometer at the Vrije Universiteit Amsterdam, The Netherlands. Analytical standard deviation for both instruments was <0.15 ‰.

### 2.3.3 Analysis of water isotopes

We measured stable isotopes of oxygen and hydrogen ( $\delta^{18}\text{O}$ ,  $\delta^2\text{H}$ ) in water to characterize the hydrological conditions in the Kolyma River and its tributaries. Samples were analyzed with a Picarro Inc L2140-i Wavelength-scanning cavity ring-down spectrometer in replicates of seven, of which the first three were discarded to avoid carry-over effects. After a sequence of 10 samples, three in-house standards, all calibrated against international IAEA standards (VSLAP and VSMOW), were analyzed. The fourth in-house standard (KONA) was used to control precision and accuracy of the measurements (standard deviation <0.1 ‰ for  $\delta^{18}\text{O}$  and <2 ‰ for  $\delta^2\text{H}$ ). The analysis was carried out at the Vrije Universiteit Amsterdam, The Netherlands.



## 110 2.4 Spatial analysis and landscape characterization

We delineated catchments using a 90 m digital elevation model (DEM) (Santoro and Strozzi, 2012) and determined mean soil OC content (SOCC) (Hugelius et al., 2013), land cover (Buchhorn et al., 2020) and calculated slope for each catchment using QGIS 3.16.1 with GRASS 7.8.4 (Fig. 1B). Prior to the spatial analysis, the DEM was pre-processed by filling all data gaps and sinks using algorithm described in Wang and Liu (2006). Two of the smallest catchments, FPS1 and FPS2, were delineated manually using a satellite image as a template, as the DEM resolution was too coarse for delineating these small and flat catchments. For the Kolyma River watershed, we used a delineation from Shiklomanov et al. (2021). Based on size and land cover, we grouped catchments into floodplain (FPS1, FPS2), headwater (Y3, Y4), tundra (Sukharnaya, Malenki Annui), wetland (Panteleikha, Ambolikha), and forest (Bolshoi Annui, Filipovkaya) stream/rivers and Kolyma mainstem as its own.

## 2.5 Source apportionment

120 For the source apportionment of POC, we used a Markov Chain Monte Carlo model to quantify contributions between autochthonous (i.e., primary production), active layer, terrestrial vegetation and permafrost sources. The source apportionment model accounts for uncertainties in the sources (i.e., endmembers), and estimates the residual error for the model (Stock and Semmens, 2016). We used a trophic discrimination factor (TDF) of zero assuming no discrimination (Stock and Semmens, 2016), and sampling year/season and river classes (e.g., tundra, headwater) as fixed effects for the model. The  $\delta^{13}\text{C}$  and  $\Delta^{14}\text{C}$  endmembers used were: autochthonous ( $\delta^{13}\text{C} -32.6 \pm 5.2 \text{‰}$ ,  $n=157$ ;  $\Delta^{14}\text{C} -43.2 \pm 79 \text{‰}$ ,  $n=79$ ), active layer ( $\delta^{13}\text{C} -26.4 \pm 0.8 \text{‰}$ ,  $n=56$ ;  $\Delta^{14}\text{C} -198 \pm 148 \text{‰}$ ,  $n=60$ ), terrestrial vegetation ( $\delta^{13}\text{C} -27.7 \pm 1.3 \text{‰}$ ,  $n=94$ ;  $\Delta^{14}\text{C} 97 \pm 125 \text{‰}$ ,  $n=58$ ) and permafrost ( $\delta^{13}\text{C} -26.3 \pm 0.7 \text{‰}$ ,  $n=414$ ;  $\Delta^{14}\text{C} -777 \pm 106 \text{‰}$ ,  $n=527$ ) according to Behnke et al. (2023), Levin et al. (2013), Vonk et al. (2012), Wild et al. (2019) and Winterfeld et al. (2015). See further details about the endmembers in Appendix A.

130 For the model prior, we used a Dirichlet distribution as an uninformative (on the simplex) prior. We used the model with a chain length of 300,000, burn-in period of 200,000 and thinning of 100. The model was run in R (R Core Team, 2020) with a package *MixSiar* (Stock and Semmens, 2016). To evaluate the model convergence, we used the Gelman-Rubin and Geweke diagnostics, as well as the deviance information criteria. We report results as a mean  $\pm$  standard deviation.

## 2.6 Statistical analyses

To test the difference in means in water chemistry parameters (water temperature, electrical conductivity - EC, pH and  $\delta^{18}\text{O}$ ) and carbon data (POC, DOC, DIC,  $\delta^{13}\text{C}$ -OC,  $\delta^{13}\text{C}$ -DIC and  $\Delta^{14}\text{C}$ -POC) between seasons (freshet vs summer) in the tributaries and the Kolyma mainstem, we used a Welch's t-test.

Additionally, we tested differences in above mentioned carbon parameters between differently sized streams/rivers during freshet and summer using analysis of variance (ANOVA). We grouped the rivers in small (FPS1, FPS2, Y3, Y4), midsized (Panteleikha, Ambolikha, Sukharnaya, Filipovkaya) and large rivers (Malenki Annui, Bolshoi Annui, Kolyma mainstem).



140 For the linear regression model of water temperature and  $\delta^{13}\text{C}$ -POC;  $\delta^{13}\text{C}$ -POC and POC-%; and  $\Delta^{14}\text{C}$ -POC and POC-%, we used a function *lm*. The same function was used for linear regression of spatial parameters (slope and SOCC) and OC concentrations. The significance level of all the statistical testing was 0.05. Testing was conducted in R (R Core Team, 2020). For further details on statistical methods, see Appendix A.

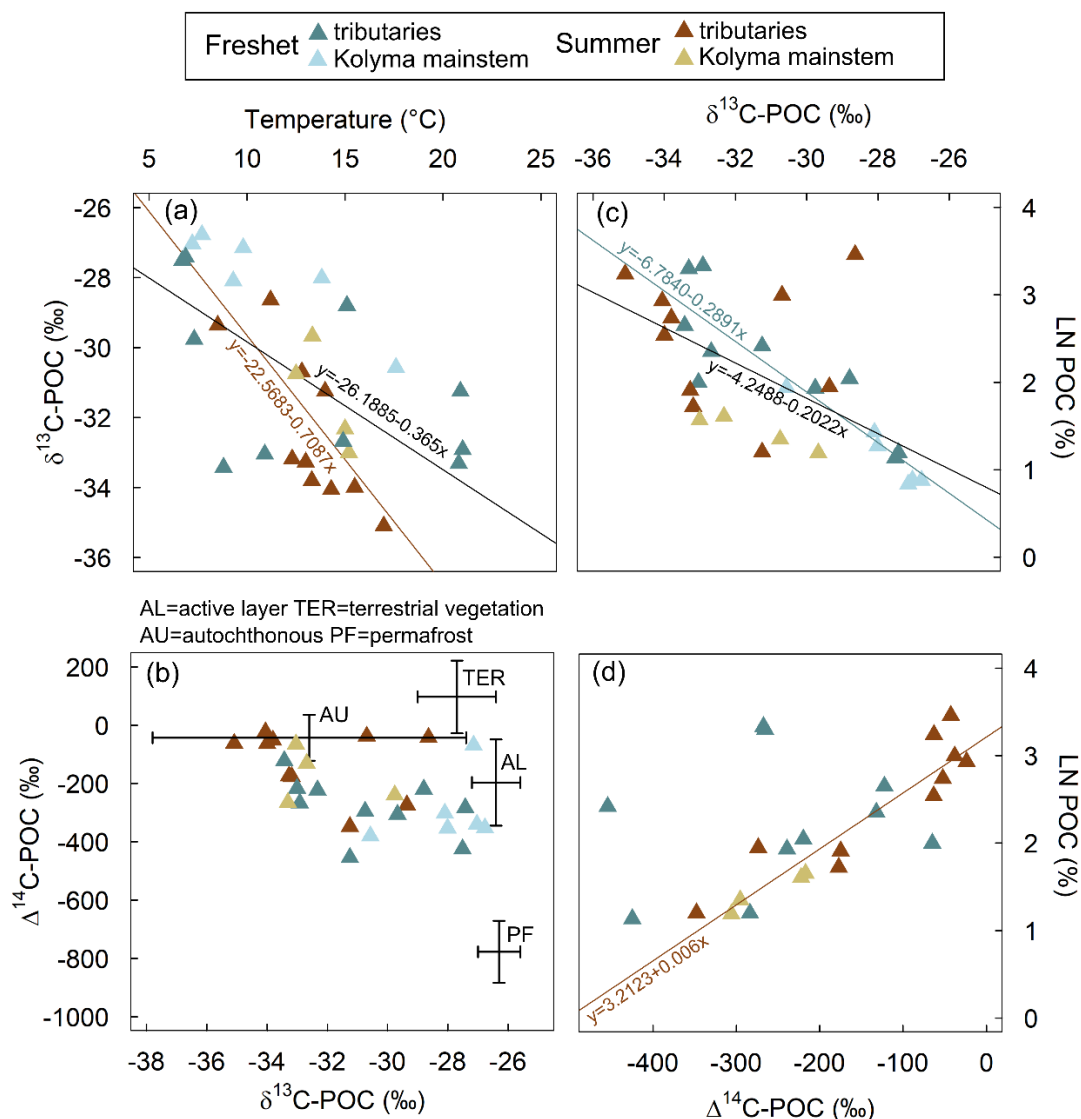
### 3 Results

145 Part of the Kolyma River mainstem data that we present here has already been reported in Keskitalo et al. (2022), including water chemistry, OC concentrations, and isotopes for organic and inorganic carbon (Tables A1, A2, A3).

#### 3.1 Catchment characteristics and water chemistry

Tributary catchments ranged in size from  $<1 \text{ km}^2$  to nearly  $60,000 \text{ km}^2$  (Table A1). Mean SOCC varied between 269 and  $414 \text{ hg C/m}^2$  with the highest SOCC in the floodplain streams (FPS1, FPS2) and lowest in the tundra river Sukharnaya (Table A1).  
150 Mean catchment slope ranged from 0.01 to  $7^\circ$  with lowest slope in the floodplain streams and highest in the tundra river Malenki Annui (Table A1). Bolshoi Annui, Filipovkaya, Y3 and Y4 were largely covered by forest (55–74 %), while Sukharnaya and Malenki Annui showed highest coverage of herbaceous vegetation (53–84 %; Fig. 1B, Table A2). The floodplain streams had the highest fraction of wetland coverage (76–80 %).

Surface water temperatures did not significantly differ between freshet and summer in the tributaries ( $p=0.946$ ) or in the  
155 Kolyma mainstem ( $p=0.126$ ) but showed a larger variability during freshet ( $6.7$  to  $21^\circ\text{C}$  in tributaries;  $7.2$  and  $18.0^\circ\text{C}$  in mainstem) than in summer ( $8.5$  to  $17^\circ\text{C}$  in tributaries;  $12.5$  to  $15.0^\circ\text{C}$  in mainstem, Fig. 2A, Table A6). The EC and water isotope ( $\delta^{18}\text{O}$ ) signature were lower during freshet than summer both in the tributaries ( $p<0.001$  and  $p<0.001$ , respectively) and the Kolyma mainstem ( $p<0.005$  and  $p=0.048$ , respectively; Tables 1, A2 and A6).



160 **Figure 2.** (a) Surface water temperature and  $\delta^{13}\text{C}$  of particulate organic carbon (POC). The linear regression for tributaries and Kolyma  
 mainstem during both freshet and summer ( $R^2=0.33$ ,  $F(1,28)=15.07$ ,  $p<0.001$ ; black line) and only during summer ( $R^2=0.49$ ,  $F(1,12)=13.58$ ,  
 $p=0.003$ ; brown line) was statistically significant while for freshet, or Kolyma mainstem and the tributaries separately, it was not. (b) The  
 $\Delta^{14}\text{C}$ -POC and  $\delta^{13}\text{C}$ -POC endmembers are indicated with arrows: OC from active layer (AL), terrestrial vegetation (TER), autochthonous  
 165 (AU) and permafrost (PF) sources. Endmembers are according to Behnke et al. (2023), Levin et al. (2013), Vonk et al. (2012), Wild et al.  
 (2019) and Winterfeld et al. (2015). See appendix A for more details about endmembers. (c) The  $\delta^{13}\text{C}$ -POC and natural logarithm (LN) of  
 POC-% (amount of POC of total suspended solids). The linear regression for the Kolyma mainstem and tributaries (both freshet and summer,  
 $R^2=0.39$ ,  $F(1,28)=19.36$ ,  $p<0.001$ ; black line) and separately for freshet was statistically significant ( $R^2=0.82$ ,  $F(1,14)=67.57$ ,  $p<0.001$ ;  
 blue line). Linear regression for summer only was not significant, or for tributaries and Kolyma mainstem separately. (d) The  $\Delta^{14}\text{C}$ -POC as  
 170 a function of LN POC-%. Linear regression for summer (both Kolyma mainstem and tributaries) was significant ( $R^2=0.85$ ,  $F(1,12)=75.4$ ,  
 $p<0.001$ ; brown line). Linear regression for the Kolyma mainstem or tributaries separately was not significant. All panels include data from  
 freshet (June 2019) and summer (July–Aug 2018) in the Kolyma River mainstem and its tributaries. Part of the Kolyma data has been  
 previously reported in Keskitalo et al. (2022).



### 3.2 Total suspended solids, carbon concentrations and isotopes of carbon

175 Concentrations of TSS were higher during freshet than summer at all sites (not statistically significant  $p=0.289$ ; Tables 1, A6) except at FPS1, FPS2 and Y3 that showed the opposite pattern. Concentrations of POC and TPN largely followed the same trend (not statistically significant,  $p=0.457$  and  $p=0.669$ , respectively; Table A6). In the Kolyma mainstem, POC concentrations were higher during freshet than summer ( $p=0.04$ ; Table A6), while TSS and TPN showed a similar pattern (not statistically significant,  $p=0.071$  and  $p=0.093$ , respectively). In the tributaries, DOC concentrations did not differ between  
180 seasons ( $p=0.242$ ), while DIC concentrations were lower during freshet than summer ( $p<0.005$ ; Table A6). In the Kolyma mainstem, DOC concentrations were higher during freshet than summer ( $p<0.005$ ) while DIC showed the opposite pattern ( $p=0.015$ ; Table A6). Of the total carbon pool (POC, DOC and DIC), POC was the smallest carbon fraction both during freshet and summer (Fig. 3, Table A7).

During freshet, large rivers showed higher TSS and lower DOC concentrations than small ones ( $p=0.007$  and  $p=0.018$ ,  
185 respectively), while POC, TPN and DIC did not differ between different sized rivers (Table A8). The POC-% (amount of OC of TSS) was higher in small and midsized rivers than larger ones during freshet ( $p=0.005$ ) and summer ( $p=0.012$ ; Fig. 4, Table A8). In summer, DOC concentrations were higher in small rivers than in large ones ( $p=0.003$ ) while TSS, POC, TPN and DIC did not differ between different sized rivers (Table A8).

In the tributaries, the  $\delta^{13}\text{C}$ -POC did not differ between seasons ( $p=0.320$ ) while  $\delta^{13}\text{C}$ -DOC were higher during freshet than  
190 in summer ( $p<0.001$ ; Table A6). In the Kolyma mainstem, both  $\delta^{13}\text{C}$ -POC ( $p=0.01$ ) and  $\delta^{13}\text{C}$ -DOC ( $p=0.005$ ; Table A6) showed higher values during freshet than summer. The  $\Delta^{14}\text{C}$ -POC were lower (i.e., older) during freshet than summer in the tributaries ( $p=0.029$ ) while in the Kolyma mainstem the trend was similar, but not statistically significant ( $p=0.94$ ; Fig. 2B, Table A6). While we did not measure  $\Delta^{14}\text{C}$ -DOC, we report previously unpublished data (May–October 2006–2011) at FPS, Y3, Y4 and Pantheleikha (Table A10) showing that all DOC is modern. The  $\delta^{13}\text{C}$ -DIC was lower during freshet than summer  
195 both in the tributaries ( $p<0.001$ ) and in the Kolyma mainstem ( $p=0.004$ ; Table A6).

During freshet, small and midsized rivers showed lower  $\delta^{13}\text{C}$ -POC than large rivers ( $p=0.001$ ) while only midsized rivers showed also lower  $\delta^{13}\text{C}$ -DOC ( $p=0.028$ ; Table A8). During summer, the  $\Delta^{14}\text{C}$ -POC was higher (i.e., younger) in the small and midsized rivers than in the large ones (only significant for the small ones  $p=0.044$ ; Fig. 4). In summer, there was no significant difference in  $\delta^{13}\text{C}$ -OC and  $\delta^{13}\text{C}$ -DIC between differently sized rivers (Table A8).

**Table 1.** Concentrations of total suspended solids (TSS), particulate and dissolved organic carbon (POC and DOC, respectively), dissolved inorganic carbon (DIC) in the tributary streams and the Kolyma River during freshet (June 2019) and summer (July–Aug 2018). Watershed types (WST) are abbreviated as headwaters (H), floodplain (FP), wetland (W), tundra (T) and forest (F). Tributary streams are abbreviated as AMB=Ambolikha, SUK=Sukharnaya, PAN=Panteleikha, FIL=Filipovkaya, MAL=Malenki Annui and BOL=Bolshoi Annui. The Kolyma mainstem is abbreviated as KOL. Also shown are stable and radioisotopes of carbon:  $\delta^{13}\text{C}$  of POC, DOC and DIC, and  $\Delta^{14}\text{C}$ -POC, and concentrations of total particulate nitrogen (TPN), molar ratio of POC/TPN and water isotopes ( $\delta^{18}\text{O}$ ,  $\delta\text{H}$ ). For DIC,  $\delta^{13}\text{C}$ -DIC,  $\Delta^{14}\text{C}$ -POC and water isotopes, mean  $\pm$  analytical standard deviation is shown. For the Kolyma River, mean  $\pm$  standard deviation between different sampling locations (freshet  $n=6$ , summer  $n=4$ ) is indicated, including standard deviation between replicate samples (Table A2) and analytical uncertainties when applicable. Additionally, we show mean (Ave)  $\pm$  standard deviation of all tributaries. Further information regarding the watersheds (e.g., size, land cover) is available in Appendix A.

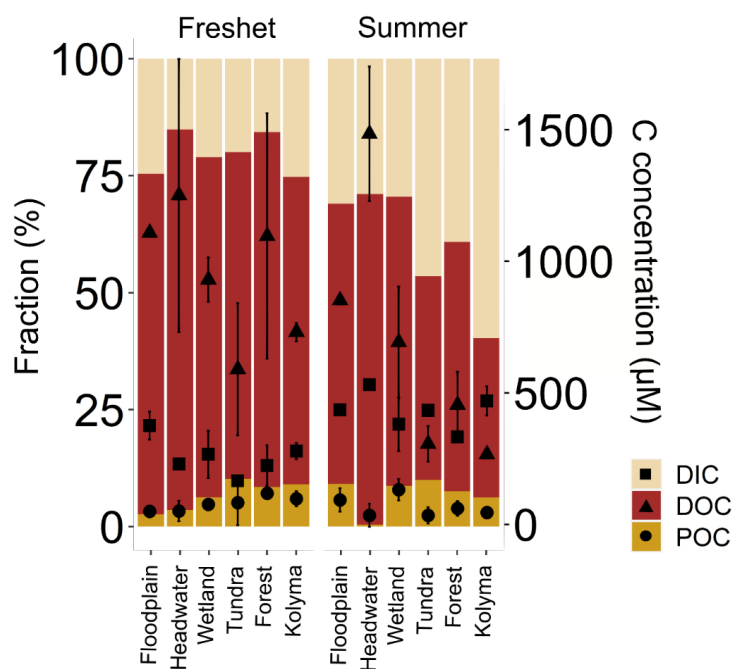
River	WST	TSS (mg/L)	POC ( $\mu\text{M}$ )	POC (%)	$\delta^{13}\text{C}$ -POC (‰)	$\Delta^{14}\text{C}$ -POC (‰)	TPN ( $\mu\text{M}$ )	POC/TPN	DOC ( $\mu\text{M}$ )	$\delta^{13}\text{C}$ -DOC (‰)	DIC ( $\mu\text{M}$ )	$\delta^{13}\text{C}$ -DIC (‰)	$\delta^{18}\text{O}$ (‰)
Y4	H	7.0	82.1	14	-33.43	-122 $\pm$ 21	8.31	8.5	887	-26.86	220 $\pm$ 9	-16.02 $\pm$ 0.1	-22.81 $\pm$ 0.1
Y3	H	4.7	26.8	6.9	-29.76	-239 $\pm$ 24	2.34	8.7	1621	-27.22	246 $\pm$ 5	-15.72 $\pm$ 0.2	-22.58 $\pm$ 0.4
FPS1	FP	4.4	40.7	11	-31.25	-454 $\pm$ 26	2.80	12.5	1110	-28.56	376 $\pm$ 16	-17.67 $\pm$ 0.3	-23.30 $\pm$ 0.0
FPS2	FP	2.8	65.9	28	-32.92	-268 $\pm$ 29	5.51	10.2	1115	-26.50	384 $\pm$ 11	-15.32 $\pm$ 0.2	-23.04 $\pm$ 0.2
AMB	W	9.5	85.4	11	-32.68	-132 $\pm$ 26	10.8	6.6	994	-29.06	334 $\pm$ 9	-18.45 $\pm$ 0.2	-22.75 $\pm$ 0.0
SUK	T	4.0	25.9	7.7	-28.80	-220 $\pm$ 21	2.73	8.1	416	-27.34	161 $\pm$ 2	-10.91 $\pm$ 0.1	-22.34 $\pm$ 0.1
PAN	W	13	77.6	7.4	-33.04	-65.1 $\pm$ 26	8.04	8.3	874	-26.86	207 $\pm$ 8	-15.93 $\pm$ 0.5	-22.64 $\pm$ 0.1
FIL	F	4.8	107	27	-33.31	-265 $\pm$ 25	11.2	8.2	1430	-28.47	282 $\pm$ 11	-12.54 $\pm$ 0.0	-22.56 $\pm$ 0.1
MAL	T	54	148	3.3	-27.42	-284 $\pm$ 27	15.7	8.1	771	-26.21	178 $\pm$ 22	-17.05 $\pm$ 0.4	-22.70 $\pm$ 0.2
BOL	F	53	138	3.1	-27.51	-425 $\pm$ 299	12.6	9.4	770	-26.44	174 $\pm$ 4	-16.66 $\pm$ 0.1	-22.88 $\pm$ 0.1
Ave	-	16 $\pm$ 20	79.5 $\pm$ 42	12 $\pm$ 8.9	-31.01 $\pm$ 2.4	-247 $\pm$ 158	8.0 $\pm$ 4.6	8.9 $\pm$ 1.6	999 $\pm$ 345	-27.35 $\pm$ 1.0	256 $\pm$ 91	-15.63 $\pm$ 2.4	-22.58 $\pm$ 4
KOL	-	39 $\pm$ 26	91.6 $\pm$ 36	3.6 $\pm$ 1.9	-27.94 $\pm$ 1.4	-299 $\pm$ 71	8.2 $\pm$ 2.9	9.4 $\pm$ 0.9	708 $\pm$ 75	-26.70 $\pm$ 0.4	283 $\pm$ 85	-13.09 $\pm$ 1.6	-22.52 $\pm$ 2
Y4	H	0.3	7.8	32	-28.64	-42.7 $\pm$ 27	0.60	11.2	1308	-29.51	535 $\pm$ 0.3	-15.27 $\pm$ 0.1	-18.61 $\pm$ 0.1
Y3	H	15	70.5	5.6	-30.65*	-177 $\pm$ 20	4.96	12.2	1670	-29.20	n/a	n/a	-20.09 $\pm$ 0.1
FPS1	FP	7.8	129	20	-30.70	-38.2 $\pm$ 18	7.15	15.5	846	-29.46	438 $\pm$ 0.2	-12.10 $\pm$ 0.0	-21.39 $\pm$ 0.1
FPS2	FP	5.1	66.2	15	-33.80	-52.3 $\pm$ 18	5.77	9.8	865	-29.72	442 $\pm$ 0.2	-8.31	-20.07 $\pm$ 0.0
AMB	W	8.1	85.8	13	-34.00	-63.2 $\pm$ 17	9.42	7.8	806	-29.38	457 $\pm$ 0.2	-12.38 $\pm$ 0.0	-21.15 $\pm$ 0.1
SUK	T	2.9	16.7	7.0	-29.36	-274 $\pm$ 24	1.44	9.9	359	-28.77	n/a	n/a	-18.97 $\pm$ 0.0
PAN	W	9.2	143	19	-34.06	-23.9 $\pm$ 18	19.0	6.5	809	-31.16	313 $\pm$ 0.1	-11.42 $\pm$ 0.1	-20.95 $\pm$ 0.0
FIL	F	4.0	84.5	25	-35.10	-62.9 $\pm$ 17	10.9	6.7	548	-29.65	328 $\pm$ 0.1	-8.02 $\pm$ 0.0	-20.48 $\pm$ 0.0
MAL	T	22	60.0	3.3	-31.25	-348 $\pm$ 18	6.29	8.2	263	-28.91	281 $\pm$ 0.1	-9.91 $\pm$ 0.1	-20.20 $\pm$ 0.1
BOL	F	8.1	45.4	6.7	-33.27	-175 $\pm$ 19	5.31	7.3	368	-29.47	346 $\pm$ 0.1	-10.60 $\pm$ 0.1	-21.01 $\pm$ 0.0
Ave	-	8.2 $\pm$ 6	70.9 $\pm$ 43	15 $\pm$ 9.4	-32.08 $\pm$ 2.2	-126 $\pm$ 129	7.1 $\pm$ 5.2	9.5 $\pm$ 2.8	784 $\pm$ 441	-29.52 $\pm$ 0.7	393 $\pm$ 88	-11.0 $\pm$ 2.4	-20.29 $\pm$ 0.9
KOL	-	15 $\pm$ 7	51.7 $\pm$ 13	4.2 $\pm$ 0.9	-31.44 $\pm$ 1.5	-273 $\pm$ 77	5.9 $\pm$ 1.1	7.6 $\pm$ 0.9	271 $\pm$ 26	-29.24 $\pm$ 0.8	473 $\pm$ 56	-9.30 $\pm$ 0.2	-21.78 $\pm$ 0.4

\*average of a tributary of Y3 and Y3 mainstem upstream of the sampling site in 2018 as  $\delta^{13}\text{C}$  analysis at the sampling location was not successful.



210

211



212 **Figure 3.** Fractions (%) of different carbon pools: particulate and dissolved organic carbon (POC and DOC, respectively) and  
 213 dissolved inorganic carbon (DIC) in the Kolyma River and its tributary rivers/streams during freshet (2019) and summer (2018).  
 214 On the right-side y-axis, concentrations of respective carbon pools are shown with square (DIC), triangle (DOC) and circle  
 215 (POC) symbols with mean  $\pm$  standard deviation between samples. The tributaries are grouped based on their land cover and  
 216 size as follows (n=2 per group per season except for the Kolyma mainstem n=6 during freshet and n=4 during summer): tundra  
 217 = Sukharnaya and Malenki Annui; headwater (small, forested watersheds) = Y3, Y4; floodplain = FPS1 and FPS2; wetland  
 218 (influenced) = Ambolikha and Panteleikha; forest (larger forested watersheds) = Filipovkaya and Bolshoi Annui; Kolyma =  
 219 Kolyma mainstem. The DIC concentrations were not measured for Sukharnaya and Y3 during summer.

220



221 **3.3 Source apportionment**

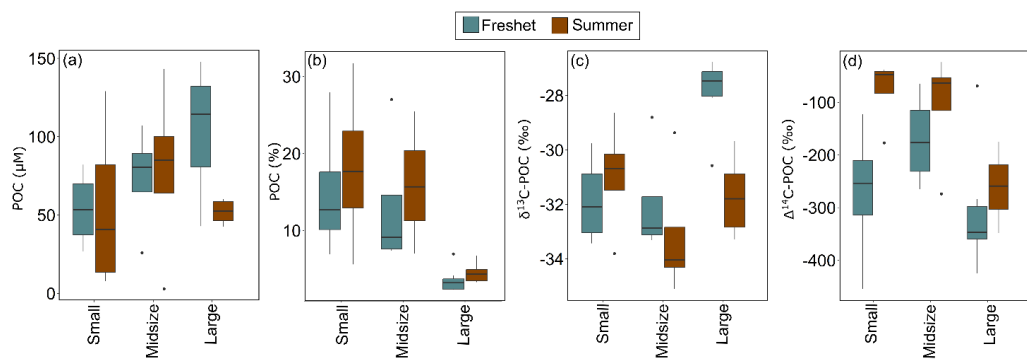
222 Both during freshet and summer, POC was largely autochthonous in the tributaries (34–82 % and 56–92 %,  
223 respectively; Fig. 5, Table A11) and in the Kolyma mainstem (35 and 59 %, respectively). Permafrost-derived  
224 POC was higher during freshet than summer at all sites (tributaries 8–33 % during freshet and 3–22 % during  
225 summer; mainstem 34 % during freshet and 22 % during summer). Contributions from active layer and terrestrial  
226 vegetation were lowest to tributary-POC (8–24 % and 4–10% during freshet, respectively; 3–16 % and 2–7 %  
227 during summer, respectively; Fig. 5) Similarly, active layer and terrestrial vegetation contributed least to the  
228 Kolyma waters during freshet (9–22 %) and summer (6–13 %; Table A11).

229 **4 Discussion**

230 **4.1 Smaller tributary streams may start primary production earlier than larger rivers in the spring**

231 In all tributaries and the Kolyma mainstem, the water isotope  $\delta^{18}\text{O}$  signature significantly differed between seasons  
232 (Table A6). Lower  $\delta^{18}\text{O}$  signal during freshet suggests that snowmelt was the dominant water source (Welp et al.,  
233 2005), supported by lower EC values (Table A6). However, water temperatures varied more within a season than  
234 between seasons both in the tributaries and in the Kolyma (Table A6). Air temperatures were particularly warm  
235 during freshet 2019 (see Fig. A2 for average air temperatures in 2007–2017) that was reflected as warm water  
236 temperatures especially in Filipovkaya and the floodplain streams ( $>20\text{ }^{\circ}\text{C}$ ). These high temperatures likely  
237 promoted a rapid onset of autochthonous production as suggested by relatively low  $\delta^{13}\text{C}$ -POC (up to  $-33.43\text{ }‰$ )  
238 for the season, combined with high POC-% (11–28 %, Fig. 2C). However, in tributaries Y4, Panteleikha and  
239 Ambolikha low  $\delta^{13}\text{C}$ -POC occurred already prior to the high air temperatures (Table A3), suggesting that other  
240 factors such as higher nutrient fluxes during freshet likely also play a role in inducing primary production (Harrison  
241 and Cota, 1991; Holmes et al., 2012; Mann et al., 2012). Water temperature explained 33 % of the variability in  
242  $\delta^{13}\text{C}$ -POC overall (higher temperature indicating lower  $\delta^{13}\text{C}$ -POC), while during summer it explained ~50 % of  
243 its variability (Fig. 2A), confirming that other factors affect  $\delta^{13}\text{C}$ -POC. Overall, freshet  $\delta^{13}\text{C}$ -POC was lower and  
244 POC-% higher in small and midsized rivers compared to the large ones (Fig. 4; Table A8), suggesting that river  
245 size may play a role in the timing for primary production onset during freshet. Higher input of (terrestrial) DOC  
246 (via degradation to inorganic carbon to be taken up by primary producers) and/or nutrients combined with shorter  
247 transport times may enhance primary production in smaller streams during freshet. In contrast, large rivers have  
248 longer transport times, and nutrients may already have been utilized (in headwaters), and terrestrially derived DOC  
249 degraded (Denfeld et al., 2013). Our POC data suggest that autochthonous production may start sooner in small  
250 and midsized tributaries than in large rivers during freshet.

251



252

253

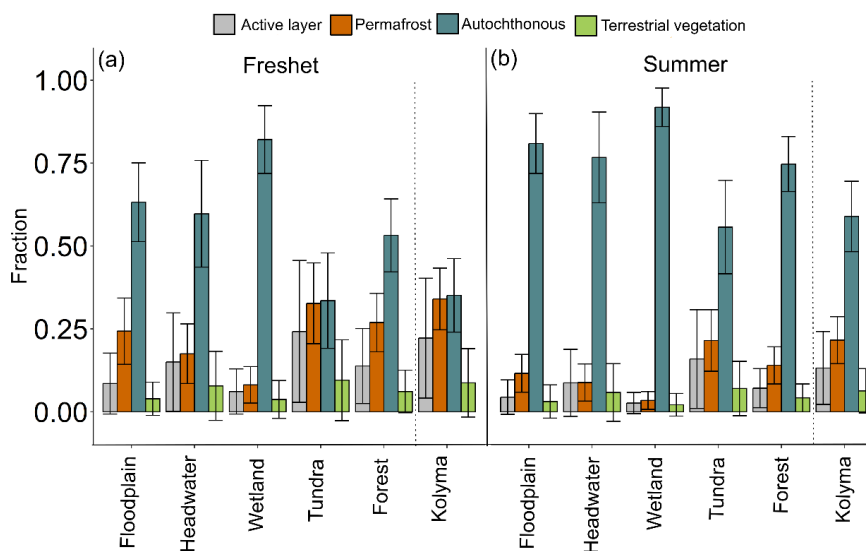
254 **Figure 4.** Concentrations of particulate organic carbon (POC) in (a)  $\mu\text{M}$  and (b) percent in small, midsize, and large rivers  
 255 during freshet and summer. The (c)  $\delta^{13}\text{C-POC}$  and (d)  $\Delta^{14}\text{C-POC}$  in small, midsize, and large rivers. Boxplots show median  
 256 (line), interquartile range (the box) and minimum and maximum (whiskers). For small rivers  $n=4$  per season, for midsize  
 257 rivers  $n=4$  per season and for large rivers  $n=7$  in summer and  $n=9$  in freshet.

258 **4.2 Organic and inorganic carbon dynamics differ between the tributaries and the Kolyma River mainstem**

259 **4.2.1 Suspended matter dynamics**

260 During freshet, mean TSS and POC concentrations were higher in the large rivers than in the small tributary rivers  
 261 (statistically significant only for TSS; Table A8) likely due to higher river power causing greater bank erosion  
 262 (delivering sediment and POC) as well as higher turbulence promoting particle suspension (Striegl et al., 2007).  
 263 Spatial characteristics such as catchment slope or SOCC did not show a linear relationship with summer-POC,  
 264 indicating that other factors, such as abrupt permafrost thaw, primary production, and water temperature, likely  
 265 play a more important role in driving POC concentrations (Fig. A3, Sect. 4.3). In the Kolyma, POC and  $\delta^{13}\text{C-POC}$   
 266 were significantly different between seasons, while in the tributaries there was no significant difference (Table  
 267 A6). This likely suggests both local variability and stronger fluctuations in the tributaries that react faster to  
 268 environmental changes such as high air temperatures.

269



270

271 **Figure 5.** Fractions of different particulate organic carbon (POC) sources (active layer, terrestrial vegetation, autochthonous  
 272 and permafrost) according to Markov Chain Monte Carlo source apportionment modelling using  $\delta^{13}\text{C}$  and  $\Delta^{14}\text{C}$  during (a)  
 273 freshet and (b) summer. The dashed lines separate the Kolyma mainstem from the tributaries. For each catchment type  
 274 (floodplain, headwater, wetland, tundra and forest)  $n=2$  for the number of tributaries per season while for the Kolyma mainstem  
 275  $n=6$  during freshet and  $n=4$  during summer. The endmembers were according to Behnke et al. (2023), Levin et al. (2013), Vonk  
 276 et al. (2012), Wild et al. (2019) and Winterfeld et al. (2015), see more information in the Appendix A.

#### 277 4.2.2 Dissolved matter dynamics

278 Previous studies have shown that lower order streams differ from the Kolyma River in their dissolved carbon  
 279 concentrations and composition (Drake et al., 2018a; Mann et al., 2012; Rogers et al., 2021). Similarly, our results  
 280 show that DOC concentrations were higher in the small tributaries than in the large ones both during freshet and  
 281 summer, while  $\delta^{13}\text{C}$ -DOC differed only between midsized and large rivers during freshet (lower for midsized  
 282 rivers; Table A8). In the tributaries, SOCC predicted nearly half of the variability in DOC concentrations during  
 283 summer (Fig. A3). It has been shown that the majority of DOC in the Kolyma mainstem originates from modern  
 284 vegetation rather than permafrost sources (Rogers et al., 2021), potentially due to rapid degradation of permafrost-  
 285 derived DOC during transit from the headwaters (Mann et al., 2015). Similarly, the  $\Delta^{14}\text{C}$ -DOC shows a modern  
 286 signal for FPS, Y4, Y3 and Panteleikha (Table A10), implying that small stream DOC is also predominantly  
 287 modern.

288 Both in the Kolyma mainstem and the tributaries, DIC and  $\delta^{13}\text{C}$ -DIC differed significantly between seasons  
 289 (Table A6) and followed a previously-reported trend in fluvial systems of lower concentrations and  $\delta^{13}\text{C}$ -DIC  
 290 during freshet than summer (Campeau et al., 2017; Waldron et al., 2007). Our Kolyma DIC concentrations were  
 291 close to a previously reported concentration (Drake et al., 2018b), while  $\delta^{13}\text{C}$ -DIC values were  $\sim 2\text{‰}$  higher in our  
 292 study. The higher DIC concentrations during summer may reflect an increase in leaching from the active layer  
 293 and/or re-mineralization of DOC, while the higher  $\delta^{13}\text{C}$ -DIC suggests primary production and/or partial  $\text{CO}_2$   
 294 evasion, where part of the  $\text{CO}_2$  is likely sourced from degraded permafrost (Campeau et al., 2017; Drake et al.,  
 295 2018b; Powers et al., 2017; Waldron et al., 2007). During freshet, DIC concentrations were higher in watersheds



296 with higher water temperatures, a trend not observed during summer (Table 1). While higher temperatures may  
297 increase CO<sub>2</sub> evasion and thus lower DIC concentrations (and increase δ<sup>13</sup>C-DIC) (Campeau et al., 2017), on-  
298 going OC degradation potentially keeps the concentrations high. The higher δ<sup>13</sup>C-DIC of the Kolyma mainstem,  
299 Sukharnaya and Filipovkaya, suggests that they may be affected by CO<sub>2</sub> evasion during turbulent freshet  
300 conditions. At Filipovkaya, these high ratios may be partially due to primary production (i.e., biological  
301 consumption of DIC) as the δ<sup>13</sup>C-POC is relatively low (Table 1). In headwater streams, contribution of OC  
302 mineralization to the DIC pool has been suggested to be negligible relative to terrestrial input (Winterdahl et al.,  
303 2016). Smaller streams have been shown to evade more CO<sub>2</sub> to the atmosphere than larger rivers during summer,  
304 thus suggesting that CO<sub>2</sub> evasion from smaller streams is mainly driven by hydrological flow paths and terrestrial  
305 OC, while in the larger rivers autochthonous production dominates as a CO<sub>2</sub> sink (Denfeld et al., 2013). Finally,  
306 weathering, dominated by carbonates and silicates in the Kolyma watershed, may add to the DIC concentrations  
307 (Tank et al., 2012).

#### 308 **4.3 The importance of autochthonous production: riverine POC dominates in the tributaries**

309 Tributary-POC is mostly autochthonous both during freshet (58 ± 33 %) and summer (76 ± 27 %) indicating high  
310 primary production, especially in summer (Fig. 5) supported by higher OC-% in small and midsized tributaries  
311 (6.9–20 % and 5.6–32 %, respectively) than in the large rivers (~3 % and 3–7 %, respectively; Tables A8). The  
312 Δ<sup>14</sup>C-POC was significantly higher (i.e., younger) in tributaries during summer than freshet, likely due to higher  
313 primary production, while in the Kolyma Δ<sup>14</sup>C-POC did not significantly differ between seasons as shown  
314 previously (Bröder et al., 2020; McClelland et al., 2016). Filipovkaya and the floodplain streams (FPS1, FPS2)  
315 showed relatively low Δ<sup>14</sup>C-POC combined with high POC-% and low δ<sup>13</sup>C-POC (Fig. 2C–D), suggesting  
316 incorporation of old CO<sub>2</sub> into biomass, likely originating from rapid degradation of permafrost-derived DOC  
317 (Drake et al., 2018b). The permafrost fraction was relatively low during summer due to dominance of primary  
318 production (Behnke et al., 2023), which was particularly pronounced in the smaller waterways (Fig. 5).

319 In an earlier incubation study, we showed that riverine-produced POC (with low δ<sup>13</sup>C-POC) in Kolyma  
320 summer waters degrades rapidly (degradation constant  $k = -0.026 \text{ day}^{-1}$ ), while terrestrially-produced POC in  
321 freshet waters did not show OC loss (Keskitalo et al., 2022). Furthermore, we showed that a lower initial δ<sup>13</sup>C-  
322 POC corresponded to a higher POC loss. Therefore, the low δ<sup>13</sup>C-POC of small and midsized streams during  
323 freshet suggests that POC may be prone to degradation, while POC degradation in the Kolyma likely lags behind  
324 as it is still dominated by terrestrially derived POC. In smaller streams, higher water temperatures may increase  
325 activity of bacterial communities potentially resulting in stronger degradation (Adams et al., 2010). Similarly,  
326 leaching of terrestrial DOC and permafrost carbon may fuel stronger degradation of OC in the smaller streams  
327 than in the larger ones (Denfeld et al., 2013).

328 While larger rivers may be able to emit more greenhouse gases than smaller ones given their size, smaller  
329 rivers/streams play an important role in CO<sub>2</sub> evasion (Denfeld et al., 2013). Smaller waterways have been shown  
330 to convey more allochthonous OC-derived CO<sub>2</sub> emissions than larger rivers (Hotchkiss et al., 2015). With the  
331 predicted earlier onset of freshet and warmer temperatures occurring earlier in the season in the future (Meredith  
332 et al., 2019; Stadnyk et al., 2021) (i.e., creating more favorable conditions both for primary production and OC  
333 degradation) lower order streams could increase CO<sub>2</sub> evasion via degradation of autochthonous POC (that likely  
334 comprises a fraction of old permafrost OC taken up by primary producers (Drake et al., 2018b), and/or enhance



335 degradation of allochthonous OC via priming effects (Hotchkiss et al., 2014). This may be particularly relevant in  
336 the Arctic, where the high proportion of allochthonous permafrost OC present during freshet could be susceptible  
337 to decomposition (Fig. 5). However, further studies are needed to decipher whether this has implications on CO<sub>2</sub>  
338 emissions in the whole system level. Furthermore, smaller rivers may transport permafrost carbon, in the form of  
339 aquatic biomass, downstream, where its signal is mixed with modern OC sources and is not detectable anymore  
340 (Drake et al., 2018b). Understanding dynamics of smaller rivers/streams is important given that river size may  
341 affect their response to environmental drivers (Battin et al., 2023). On the whole, the intensification of hydrological  
342 cycling could mean that in the future processes currently happening in lower order streams may shift towards  
343 larger fluvial systems.

#### 344 **5 Conclusions and implications**

345 Here, we present seasonal contrasts in water chemistry and carbon characteristics of lower order streams and the  
346 Kolyma mainstem. However, during freshet small and mid-sized streams/rivers are more dynamic and seem to  
347 respond faster to environmental changes such as air temperature increases. While POC concentrations did not  
348 significantly differ between large and small/mid-sized rivers during freshet, composition of POC showed clear  
349 differences: the  $\delta^{13}\text{C}$ -POC was lower and POC-% higher in small and mid-sized streams/rivers than in large ones,  
350 indicating an early onset of primary production in these lower order streams. This may fuel CO<sub>2</sub> evasion via  
351 degradation of autochthonous POC that is likely partly comprised of permafrost OC and/or prime degradation of  
352 allochthonous OC, however, further studies are needed to discern implications on CO<sub>2</sub> emissions in a system level.  
353 Furthermore, hydrological intensification may increase shunting and decomposition of organic matter from smaller  
354 to larger river systems, and transport permafrost-derived OC downstream in the form of autochthonous POC. An  
355 increased understanding of carbon and water chemistry of lower order streams and their linkages to hydrology is  
356 therefore crucial to understand catchment-wide OC dynamics.

357



358 **Appendix A**

359 **Text A1. Representativeness of surface water samples**

360 As all our samples were of surface water, we compared our Kolyma River  $\delta^{13}\text{C}$ -POC data to Arctic Great Rivers  
361 Observatory (Arctic-GRO) to assess how our surface water samples would compare to depth-integrated sampling  
362 (data and sampling protocol are available in [www.arcticgreatrivers.com/data](http://www.arcticgreatrivers.com/data), water quality) carried out since 2003  
363 in the Kolyma River mainstem. All the water samples collected during 2003–2011 (programs PARTNERS,  
364 ARCTIC-GRO I) were depth-integrated, while samples collected between 2012 and 2021 (programs ARCTIC-  
365 GRO II-IV; data from 2020–2021 is provisional) are a combination of samples collected from the surface and at  
366 depth (sampled at depths of 4–15 m). The Arctic-GRO average  $\pm$  std  $\delta^{13}\text{C}$ -POC for freshet (sampled in June 2004–  
367 2021) was  $-28.2 \pm 1.4$  ‰ (n=19) and for summer (sampled in July–August 2003–2021) was  $-29.8 \pm 2.1$  ‰ (n=19).  
368 In comparison, our Kolyma River mainstem  $\delta^{13}\text{C}$ -POC sampled during freshet (June 2019) was  $-27.94 \pm 1.4$  ‰  
369 (n=6) and in summer (July–August 2018) was  $-31.44 \pm 1.5$  ‰ (n=4; table A2). Given that our  $\delta^{13}\text{C}$ -POC signature  
370 falls within the standard deviation of the depth-integrated samples we consider our samples to be sufficiently  
371 representative for the entire water column.

372

373 **Text A2. Endmembers for the source apportionment**

374 The endmember for autochthonous POC was according to Wild et al. (2019;  $\delta^{13}\text{C}$   $-30.6 \pm 3$  ‰, n=24), Winterfeld  
375 et al. (2015;  $\delta^{13}\text{C}$   $-30.5 \pm 2.5$  ‰, n=n/a), Levin et al. (2013;  $\Delta^{14}\text{C}$   $-39.6 \pm 5.5$  ‰, n=73) and Behnke et al. (2023;  
376  $\delta^{13}\text{C}$   $-33.1 \pm 4.7$  ‰,  $\Delta^{14}\text{C}$   $106 \pm 164$  ‰) combined with our own POC sample collected at the Panteleikha River  
377 during an algal bloom in 2019 ( $\Delta^{14}\text{C}$   $-26$  ‰;  $\delta^{13}\text{C}$   $-33.5$  ‰, n=1). The  $\delta^{13}\text{C}$  endmember values from Wild et al.,  
378 (2019) and Winterfeld et al., (2015) are of riverine phytoplankton from Ob and Yenisei rivers, and from Lena  
379 River, respectively, while the values from Levin et al. (2013) are of atmospheric  $\text{CO}_2$  (May–August 2009–2012).  
380 Endmember values from Behnke et al. (2023) are (mostly benthic) of biofilms, algae and invertebrates from  
381 Alaska, Canada, and Svalbard. As our samples were of surface water, we combined the  $\Delta^{14}\text{C}$  of atmospheric  $\text{CO}_2$   
382 from Levin et al. (2013) (following the approach used by Winterfeld et al., 2015 and Wild et al., 2019) with the  
383  $\Delta^{14}\text{C}$  of biofilms, algae, and invertebrates (following Behnke et al., 2023) as the autochthonous endmember. The  
384 autochthonous  $\delta^{13}\text{C}$  endmember was a compilation of phytoplankton (Winterfeld et al. 2015 and Wild et al. 2019)  
385 and biofilms, algae, and invertebrates (Behnke et al., 2023). For the active layer and terrestrial vegetation  
386 endmember, we used the endmembers compiled in Wild et al., (2019): endmember for active layer ( $\Delta^{14}\text{C}$   $-197.5 \pm$   
387  $148.4$  ‰, n=60;  $\delta^{13}\text{C}$   $-26.4 \pm 0.8$  ‰, n=56) and modern vegetation ( $\Delta^{14}\text{C}$   $97 \pm 124.8$  ‰, n=58;  $\delta^{13}\text{C}$   $-27.7 \pm 1.3$   
388 ‰, n=94) The active layer and terrestrial vegetation endmembers include data from Siberia, Alaska, northern  
389 Canada, and Scandinavia. For the permafrost endmember, we combined the Ice Complex Deposit ( $\Delta^{14}\text{C}$   $-954.8 \pm$   
390  $65.8$  ‰, n=329) and Holocene permafrost ( $\Delta^{14}\text{C}$   $-567.5 \pm 156.7$  ‰, n=138) endmember from Wild et al. (2019)  
391 with the Holocene permafrost endmember from Winterfeld et al. (2015;  $\Delta^{14}\text{C}$   $282 \pm 133$  ‰, n=60;  $\delta^{13}\text{C}$   $-26.6 \pm 1$   
392 ‰, n=40) and Vonk et al. (2012;  $\delta^{13}\text{C}$   $-26.3 \pm 0.7$  ‰, n=374). All endmembers were weighed with the number of  
393 observations. We recognize that having robust endmember values is important for the best modelling results, and  
394 ideally these values would come from within or close to the studied system. While the permafrost, active layer and  
395 terrestrial vegetation endmembers are relatively well defined, scientific literature lacks well-constrained  
396 autochthonous endmembers, especially for phytoplankton. Endmembers were recently discussed in Behnke et al.  
397 (2023).



398

399 **Text A3. Statistical analyses: assumptions and hypotheses**

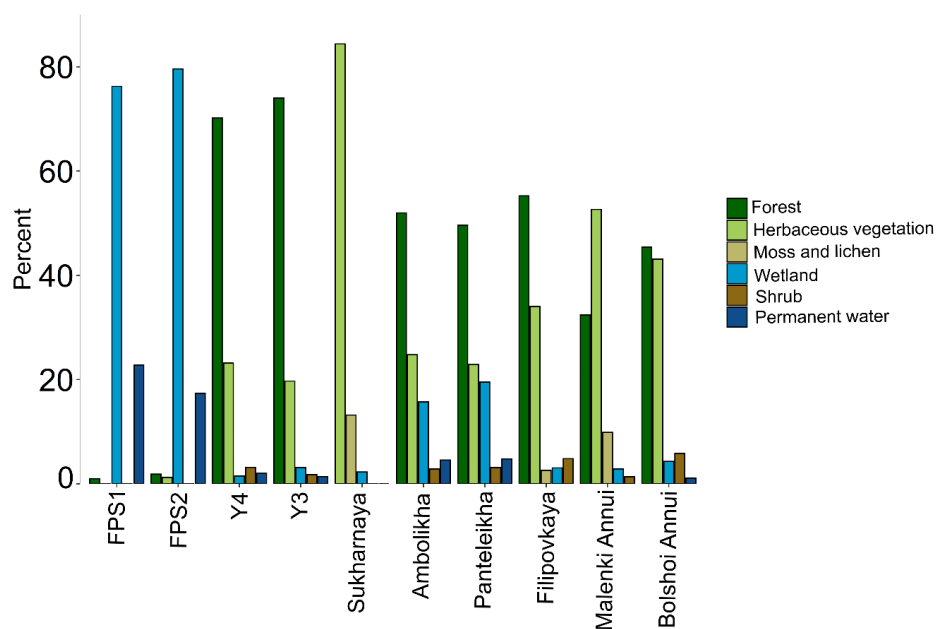
400 To test the difference in means in water chemistry parameters (water temperature, electrical conductivity - EC, pH  
401 and  $\delta^{18}\text{O}$ ) and carbon data (POC, DOC, DIC,  $\delta^{13}\text{C}$ -OC,  $\delta^{13}\text{C}$ -DIC and  $\Delta^{14}\text{C}$ -POC) between seasons (i.e., freshet  
402 and summer) in the tributaries and the Kolyma River, we used a (two-sided) Welch's t-test. Our H0 hypothesis  
403 was that the means are equal between seasons and the H1 hypothesis that the means are not equal. The test  
404 significance level was 0.05. We checked the normality of the data by using the Shapiro-Wilk test and log-  
405 transformed the data in case of non-normality. For  $\Delta^{14}\text{C}$ -POC of tributaries, a Mann-Whitney U test was used.

406 To test whether there was a significant difference between small streams, midsized rivers, and large rivers  
407 regarding carbon parameters (POC, DOC, DIC,  $\delta^{13}\text{C}$ -OC,  $\delta^{13}\text{C}$ -DIC and  $\Delta^{14}\text{C}$ -POC), we used (one-way) analysis  
408 of variance (ANOVA) or a Kruskal-Wallis test. The floodplain streams (FPS1 and FPS2), Y3 and Y4 were classed  
409 as small streams; Panteleikha, Ambolikha, Filipovkaya and Sukarnaya as midsized rivers; and Malenki Annui,  
410 Bolshoi Annui and Kolyma mainstem as large rivers. We checked the assumptions of normality and equal  
411 variances visually and further with Shapiro-Wilk test and Breusch-Pagan test, respectively. Our H0 hypothesis  
412 was that the means are equal between different sized rivers/streams and the H1 hypothesis that the means are not  
413 all equal. With significant results, we used a Tukey's test as a *post hoc* test for ANOVA and a Dunn's test for the  
414 Kruskal-Wallis test. The significance level of all the tests was 0.05.

415 For the linear regression model of water temperature and  $\delta^{13}\text{C}$ -POC;  $\delta^{13}\text{C}$ -POC and POC-%; and  $\Delta^{14}\text{C}$ -POC  
416 and POC-%, we used a function *lm*. The same function was used for linear regression of spatial parameters (slope  
417 and soil organic carbon concentration - SOCC) and OC concentrations. The POC concentrations did not show a  
418 linear relationship with the spatial parameters, thus they were not modelled. We log transformed the DOC data  
419 prior to executing the model as well as the POC-%. For all the linear regression models, we checked the  
420 assumptions of normality and homoskedasticity of the model residuals visually and using a Shapiro-Wilk test and  
421 a Breusch-Pagan test, respectively. The significance level of the test was 0.05. All the statistical testing was  
422 executed in R (R Core Team, 2020).

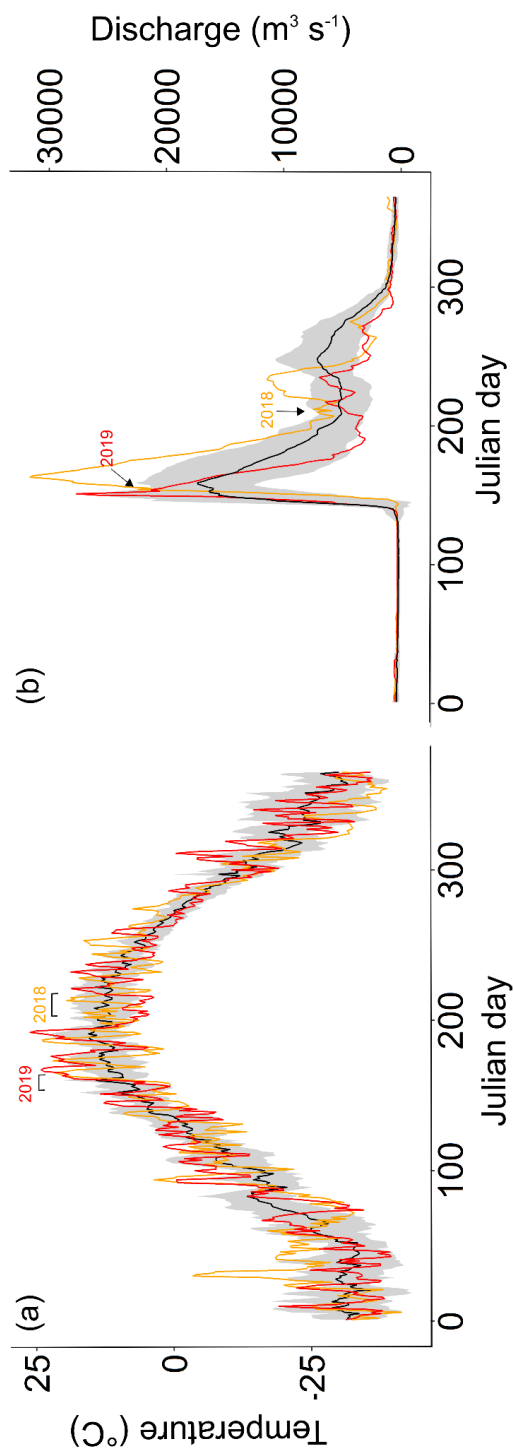
423

424

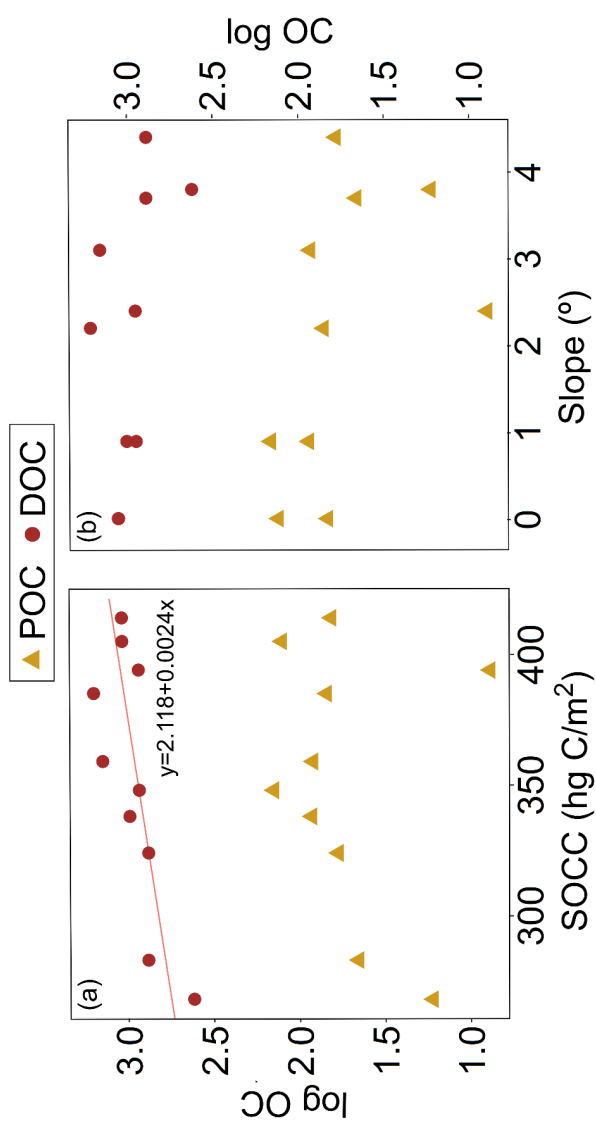


425  
426  
427  
428

**Figure A1.** Land cover of the tributary watersheds. The watersheds are organized by their size starting from the smallest (FPS1) on the left. The land cover types with < 1 % contribution are not included in the figure, see Table A5 for full land cover data.



429 **Figure A2.** (a) average air temperature  $\pm$  standard deviation (black line  $\pm$  grey background) 2007–2017 in Cherskiy with air temperatures during the sampling years 2018 (orange line) and 2019  
430 (red line). The weather data was retrieved from the Cherskiy weather station. Timing of the sampling campaigns is marked above the plot. See Table S3 for air temperatures on sampling days. (b)  
431 The average  $\pm$  standard deviation of discharge measured at Kolymnskoye 2007–2017 (Shiklomanov et al., 2021). Red line shows the discharge of the year 2019 and orange line the year 2018. The  
432 timing of the sampling campaigns is marked with arrows above the plot.  
433  
434



435  
436 **Figure A3.** (a) Particulate and dissolved organic carbon (POC and DOC, respectively) concentration (log) and soil organic carbon content (SOCC). Linear regression for DOC was statistically  
437 significant ( $R^2=0.49$ ,  $F(1,8)=9.59$ ,  $p=0.001$ ). (b) Concentrations (log) of POC and DOC against median slope. The regression model did not show statistically significant results. All the organic  
438 carbon data are from the Kolyma River tributaries sampled during summer 2018.



439 **Table A1.** Sampling coordinates and dates of the Kolyma tributaries and Kolyma mainstem during spring freshet (2019) and  
 440 summer (2018) sampling campaigns. Data from sites KOL1–KOL4 during freshet and KOL1–KOL3 during summer were  
 441 previously reported in Keskitalo et al. (2022).  
 442

Freshet	Latitude	Longitude	Sampling date (dd/mm/yyyy)
FPS1	N68.65100	E161.36472	18/06/2019
FPS2	N68.64977	E161.36742	18/06/2019
Y4	N68.74133	E161.41393	08/06/2019
Y3	N68.75919	E161.44769	09/06/2019
Sukharnaya	N69.49534	E161.83316	11/06/2019
Ambolikha	N68.66421	E161.38884	14/06/2019
Panteleikha	N68.70052	E161.52057	10/06/2019
Filipovkaya	N68.92067	E161.64552	16/06/2019
Malenki Annui	N68.47034	E160.83749	07/06/2019
Bolshoi Annui	N68.46519	E160.80356	07/06/2019
KOL1	N68.51782	E160.98093	07/06/2019
KOL2	N68.66630	E161.19991	07/06/2019
KOL3	N69.20045	E161.44044	11/06/2019
KOL4	N69.62680	E162.21594	11/06/2019
KOL3re*	N69.20045	E161.44044	16/06/2019
KOL4re*	N69.62680	E162.21594	16/06/2019
<b>Summer</b>			
FPS1	N68.65108	E161.36438	07/08/2018
FPS2	N68.64903	E161.36606	09/08/2018
Y4	N68.74216	E161.41379	04/08/2018
Y3	N68.75919	E161.44769	26/07/2018
Sukharnaya	N69.49577	E161.83197	28/07/2018
Ambolikha	N68.67504	E161.41608	21/07/2018
Panteleikha	N68.67068	E161.52295	30/07/2018
Filipovkaya	N68.90665	E161.68976	06/08/2018
Malenki Annui	N68.45193	E160.81279	01/08/2018
Bolshoi Annui	N68.46015	E160.78267	01/08/2018
KOL1	N68.50713	E160.61034	23/07/2018
KOL2	N68.75443	E161.27150	25/07/2018
KOL3	N69.20045	E161.44044	28/07/2018
KOL4	N69.32058	E161.56134	28/07/2018

443

\*repeat measurement.



444 **Table A2.** Concentrations of total suspended solids (TSS), particulate and dissolved organic carbon (POC and DOC, respectively), dissolved inorganic carbon (DIC) in the Kolyma River during  
 445 freshet (June 2019) and summer (July–Aug 2018). Also shown are stable isotopes of carbon:  $\delta^{13}\text{C}$  of POC, DOC and DIC, and concentrations of total particulate nitrogen (TPN) and molar ratio of  
 446 POC/TPN. For  $\Delta^{14}\text{C}$ -POC, see Table A7. Mean and standard deviation between replicate samples (n=4) is shown for freshet sites KOL1–KOL4 and for summer KOL1–KOL3 (n=3, KOL3 n=4)  
 447 including analytical uncertainty for DIC and  $\delta^{13}\text{C}$ -DIC. For water isotopes ( $\delta^{18}\text{O}$ ,  $\delta\text{H}$ ) and summer DIC and  $\delta^{13}\text{C}$ -DIC only analytical error (no replicates) is shown. All data from KOL1–KOL4  
 448 during freshet and KOL1–KOL3 during summer (except DIC concentrations) were previously published in Keskiäho et al. (2022).

Site	TSS ( $\text{mg L}^{-1}$ )	POC ( $\mu\text{M}$ )	POC (%)	$\delta^{13}\text{C}$ -POC (‰)	TPN ( $\mu\text{M}$ )	POC/ TPN	DOC ( $\mu\text{M}$ )	$\delta^{13}\text{C}$ -DOC (‰)	DIC ( $\mu\text{M}$ )	$\delta^{13}\text{C}$ -DIC (‰)	$\delta^{18}\text{O}$ (‰)	$\delta\text{H}$ (‰)
KOL1	51±2	103±5	2.4±0.2	-26.77±0.2	9.03±0.4	9.8±0.3	731±7	-26.36±0.2	294±18	-12.19±0.16	-22.89±0.09	-178.4±0.6
KOL2	63±5	126±4	2.4±0.2	-27.04±0.2	10.9±0.6	10±0.3	764±11	-26.42±0.2	239±16	-13.77±0.09	-22.88±0.22	-176.5±1.4
KOL3	68±2	130±5	2.3±0.1	-27.15±0.2	11.0±0.5	10±0.3	694±8	-27.11±0.2	324±10	-13.81±0.36	-22.65±0.05	-174.5±0.2
KOL4	25±2	87.4±5	4.2±0.4	-28.10±0.2	8.13±0.5	9.2±0.3	776±11	-26.89±0.1	273±8	-13.62±0.04	-22.99±0.02	-177.1±0.4
KOL3re	14	42.8	7.0	-28.01	3.92	9.4	574	-26.57	n/a	n/a	-26.57±0.26	-174.5±1.5
KOL4re	10	60.1	3.3	-30.57	6.35	8.1	710	-26.84	285±0.7	-12.07±0.1	-26.84±0.25	-169.3±1.5
KOL1	9.8	42.6±3	4.8	-33.01±0.4	4.93±0.4	7.4±0.2	262±5	-29.37±0.2	470±0.1	-9.36±0.02	-22.14±0.03	-171.7±0.7
KOL2	12±1	48.6±2	5.0±0.3	-32.32±0.6	6.20±0.3	6.7±0.1	272±15	-29.31±0.3	531±0.1	-9.46±0.04	-22.10±0.04	-171.5±0.3
KOL3	21±4	56.8±9	3.3±0.1	-29.67±0.3	5.63±0.6	8.6±0.5	278±19	-29.46±0.6	419±0.2	-9.08±0.02	-21.36±0.03	-165.5±0.1
KOL4	18	59.0	3.9	-30.75	6.72	7.5	269	-28.83	n/a	n/a	-21.53±0.02	-166.9±1.9

449

450



451 **Table A3.** Water chemistry parameters including water temperature (Water temp), dissolved oxygen (DO), electrical  
 452 conductivity (EC) and pH in the Kolyma River and its tributary streams/rivers during freshet (early June 2019) and summer  
 453 (July–Aug 2018). Also shown is air temperature (Air temp) on the sampling day measured at Cherskiy weather station. All  
 454 data from KOL1–KOL4 during freshet and KOL1–KOL3 during summer were previously published in Keskitalo et al. (2022).  
 455

<b>Freshet</b>	<b>Water temp (° C)</b>	<b>DO (mg L<sup>-1</sup>)</b>	<b>EC (µM cm<sup>-1</sup>)</b>	<b>pH</b>	<b>Air temp (° C)</b>
FPS1	20.9	3.43	46.5	7.74	19.6
FPS2	21.0	7.48	55.5	7.21	19.6
Y4	8.8	10.2	48.4	8.77	4.9
Y3	7.3	10.8	43.4	7.90	14.1
Sukharnaya	15.1	9.7	25.2	6.93	19.3
Ambolikha	14.9	7.77	48.3	7.23	21.2
Panteleikha	10.9	9.12	46	7.00	18.9
Filipovkaya	20.8	8.81	42	n/a	24.3
Malenki Annui	6.87	10.0	41.6	6.87	7.6
Bolshoi Annui	6.70	10.1	42.1	7.06	7.6
KOL1	7.70	10.5	102.00	7.10	7.6
KOL2	7.20	10.4	73.10	6.92	7.6
KOL3	9.80	9.86	68.70	6.65	19.3
KOL4	9.30	10.1	81.70	7.09	19.3
KOL3re*	13.8	9.39	104	n/a	24.3
KOL4re*	17.6	9.45	78	n/a	24.3
<b>Summer</b>	<b>Temp (° C)</b>	<b>DO (mg L<sup>-1</sup>)</b>	<b>EC (µM cm<sup>-1</sup>)</b>	<b>pH</b>	<b>Air temp (° C)</b>
FPS1	12.8	3.73	139	6.61	4.2
FPS2	13.3	9.08	180	7.26	10.1
Y4	11.2	6.36	271	7.17	14.6
Y3	12.3	6.29	211	6.98	12.8
Sukharnaya	8.5	9.63	75	7.77	7.8
Ambolikha	15.5	7.83	134	7.32	17.1
Panteleikha	14.3	8.32	139	6.93	9.2
Filipovkaya	17.0	10.1	162	7.47	7.6
Malenki Annui	14.0	9.41	185	7.09	19.1
Bolshoi Annui	13.0	8.95	169	7.06	19.1
KOL1	15.2	9.25	255	7.69	19.4
KOL2	15.0	9.43	249	7.16	13.2
KOL3	13.3	9.00	222	7.48	7.8
KOL4	12.5	9.16	228	7.25	7.8

456 \*repeat samples of KOL3 and KOL4 taken on the 16<sup>th</sup> of June 2019.

457

458



459 **Table A4.** Watershed size, slope and soil organic carbon content (SOCC) in the top 100 cm (Hugelius et al., 2013). Slope and  
460 SOCC are shown as mean  $\pm$  standard deviation, also the slope median is shown.  
461

River/stream	Watershed size (km <sup>2</sup> )	Slope mean (°)	Slope median (°)	Mean SOCC (hg C/m <sup>2</sup> )
FPS1	0.33	0.01 $\pm$ 0	0.01	405 $\pm$ 10
FPS2	0.74	0.01 $\pm$ 0	0.01	414
Y4	2.48	2.3 $\pm$ 1.6	2.4	394 $\pm$ 11
Y3	36.09	2.8 $\pm$ 3.3	2.2	385 $\pm$ 3
Sukharnaya	956.0	5.7 $\pm$ 5.6	3.8	269 $\pm$ 124
Ambolikha	1234	2.6 $\pm$ 4.9	0.9	338.3 $\pm$ 116
Panteleikha	1782	2.5 $\pm$ 4.6	0.9	355 $\pm$ 103
Filipovkaya	1966	4.4 $\pm$ 4.2	3.1	357 $\pm$ 99
Malenki Annui	49754	7.0 $\pm$ 7.4	4.4	319 $\pm$ 103
Bolshoi Annui	56636	6.2 $\pm$ 7.1	3.7	281 $\pm$ 113
Kolyma*	657171	7.8 $\pm$ 14	5.3	290 $\pm$ 188

\*Kolyma delineation from Shiklomanov et al. (2021).

462

463



464 **Table A5.** Land cover types per watershed in percentages (%). Land cover classes are according to Buchhorn et al. (2020).

465

River/Stream	Forest	Wetland	Shrubs	Herbaceous vegetation	Permanent Water	Moss and lichen	Bare sparse vegetation	Urban built
FPS1	1	76	0	0	23	0	0	0
FPS2	2	80	0	1	17	0	0	0
Y4	70	1	3	23	2	0	0	0
Y3	74	3	2	20	1	0	0	0
Sukharnaya	0	2	<1	84	<1	13	0	0
Ambolikha	52	16	3	25	5	<1	0	0
Panteleikha	50	20	3	23	5	<1	0	<1
Filipovkaya	55	3	5	34	<1	3	0	0
Malenki Annui	32	3	1	53	<1	10	<1	<1
Bolshoi Annui	45	4	6	43	1	<1	<1	<1

466

467



**Table A6.** Welch's t-test results for difference in means in electrical conductivity (EC), water temperature (Temp), pH, water isotope  $\delta^{18}\text{O}$ , total suspended solids (TSS), particulate and dissolved organic carbon (POC and DOC), dissolved inorganic carbon (DIC),  $\delta^{13}\text{C}$  of POC, DOC and DIC and  $\Delta^{14}\text{C}$ -POC between seasons (freshet and summer) in the Kolyma mainstem and its tributaries. The significantly different results are highlighted in bold. The significance level was 0.05. For  $\Delta^{14}\text{C}$  in tributaries, Mann-Whitney U test was used. See more details in the supplementary methods.

Site	EC	Temp	$\delta^{18}\text{O}$	TSS	POC	$\delta^{13}\text{C}$ -POC	$\Delta^{14}\text{C}$	TPN	DOC	$\delta^{13}\text{C}$ -DOC	DIC	$\delta^{13}\text{C}$ -DIC
Tributaries	t(9.4)= 7.36	t(11.6)= -0.07	t(18.4)= 7.19	t(17.7)= -0.92	t(17.7)= -0.76	t(17.3)= -1.13	U=79 <b>p=&lt;0.029*</b>	t(17.7)= -0.434	t(17.0)= -1.21	t(15.0)= -4.6	t(13.6)= 3.86	t(15.0)= 4.28
	<b>p=&lt;0.001*</b>	p=0.946	<b>p=&lt;0.001*</b>	p=0.371	p=0.457	p=0.274		p=0.669	p=0.242	<b>p=&lt;0.001*</b>	<b>p=&lt;0.005*</b>	<b>p=&lt;0.001*</b>
Kolyma	t(6.2)= -15.3	t(6.4)= -1.8	t(8.0)= -2.33	t(5.6)= 2.22	t(5.7)= 2.69	t(6.2)= 3.7	t(3.7)= -0.1	t(6.1)= 1.989	t(5.1)= 14.6	t(6.8)= 13.6	t(2.8)= -5.4	t(3.3)= -7.4
	<b>p=&lt;0.005*</b>	p=0.126	<b>p=0.048*</b>	p=0.071	<b>p=0.04*</b>	<b>p=0.01*</b>	p=0.94	p=0.093	<b>p=&lt;0.005*</b>	<b>p=&lt;0.005*</b>	<b>p=0.015*</b>	<b>p=0.004*</b>

468  
469  
470  
471

472  
473



474 **Table A7.** Fractions (%) of different carbon pools, particulate organic carbon (POC), dissolved organic carbon (DOC) and  
475 dissolved inorganic carbon (DIC), during freshet (June 2019) and summer (July–August 2018).  
476

River/Stream	Freshet			Summer		
	POC	DOC	DIC	POC	DOC	DIC
Floodplain	3.66	76.4	30.2	7.01	61.4	31.6
Headwater	3.53	81.3	15.1	0.42	70.7	28.9
Wetland	6.26	72.7	21.0	8.76	61.8	29.5
Tundra	10.2	69.8	20.0	9.94	43.6	46.5
Forest	8.44	75.9	15.7	7.56	53.3	39.2
Kolyma	9.05	65.7	25.3	6.24	34.2	59.6

477



**Table A8.** Analysis of variance (ANOVA) and Kruskal-Wallis test results for difference in means in total suspended solids (TSS), particulate and dissolved organic carbon (POC and DOC), total particulate nitrogen (TPN), dissolved inorganic carbon (DIC),  $\delta^{13}\text{C}$  of POC, DOC and DIC and  $\Delta^{14}\text{C}$ -POC between small rivers (FPS1, FPS2, Y3, Y4), mid-sized (mid) rivers (Panteleikha, Ambolikha, Sukharmaya, Filipovkaya) and large rivers (Malenki Annui, Bolshoi Annui and Kolyma mainstem) during freshet and summer with F statistics (from ANOVA) or H statistics (from Kruskal-Wallis test), degrees of freedom and p-values. The statistically significant ( $p < 0.05$ ) results are highlighted in bold. When ANOVA or Kruskal-Wallis test results were significant, post hoc test (Tukey's test for ANOVA and Dunn's test for the Kruskal-Wallis test) was conducted and their results (p-values) are listed below to indicate whether the difference was between small and midsize rivers, small and large rivers and/or midsize and large rivers. See more details in the supplementary methods.

	TSS	POC	POC-%	$\delta^{13}\text{C}$ -POC	$\Delta^{14}\text{C}$	TPN	DOC	$\delta^{13}\text{C}$ -DOC	DIC	$\delta^{13}\text{C}$ -DIC
<b>Freshet</b>	H(2)= p=1.000	H(2)= n/a	H(2)= p=1.000	H(2)= p=1.00	H(2)= n/a	F(1,3,2)= n/a	H(2)= p=0.704	H(2)= p=1.000	F(1,2,2)= n/a	H(2)= n/a
Small-mid		n/a	p=1.000	n/a	n/a	n/a	p=0.704	p=1.000	n/a	n/a
Small-large	<b>p=0.007</b>	n/a	<b>p=0.034</b>	n/a	n/a	n/a	<b>p=0.018</b>	p=0.369	n/a	n/a
Mid-large	p=0.069	n/a	<b>p=0.016</b>	n/a	n/a	n/a	p=0.510	<b>p=0.030</b>	n/a	n/a
<b>Summer</b>	H(2)= n/a	H(2)= n/a	H(2)= p=1.000	F(1,1,2)= n/a	H(2)= p=1.000	H(2)= n/a	H(2)= p=0.452	H(2)= n/a	F(8,2)= n/a	F(8,2)= n/a
Small-mid		n/a	p=1.000	n/a	p=1.000	n/a	p=0.452	n/a	n/a	n/a
Small-large	n/a	n/a	<b>p=0.044</b>	n/a	<b>p=0.044</b>	n/a	<b>p=0.003</b>	n/a	n/a	n/a
Mid-large	n/a	n/a	<b>p=0.034</b>	n/a	p=0.179	n/a	p=0.269	n/a	n/a	n/a

478  
479  
480  
481  
482  
483  
484

485  
486  
487



488 **Table A9.** Radiocarbon measurements for particulate organic carbon (POC) including the fraction modern (Fm),  $\Delta^{14}\text{C}$  and uncalibrated  $^{14}\text{C}$   
 489 ages. The ETH code is a unique analysis ID assigned for each sample analyzed at the Laboratory of Ion Beam Physics, ETH, Zürich. The  
 490 uncertainties are according to the method described in Haghypour et al. (2019).  
 491

	Site	ETH code	Fm	$\Delta^{14}\text{C}$	Age (yrs)
<b>Freshet</b>	FPS1	105814.1.1	0.55±0.01	-454	4800
	FPS2	105803.1.1	0.74±0.02	-268	2434
	Y4	105809.1.1	0.88±0.01	-122	982
	Y3	105811.1.1	0.77±0.01	-239	2132
	Sukharnaya	105804.1.1	0.79±0.01	-220	1927
	Ambolikha	105810.1.1	0.88±0.02	-132	1070
	Panteleikha	105813.1.1	0.94±0.02	-65	473
	Filipovkaya	105817.1.1	0.74±0.01	-265	2410
	Malenki Annui	105808.1.2	0.72±0.01	-284	2613
	Bolshoi Annui	n/a	0.58±0.17	-291	2694
	KOL1	105801.1.1	0.62±0.01	-385	3844
	KOL1 replicate 1	105813.1.2	0.68±0.01	-321	3047
	KOL2	105811.1.2	0.66±0.01	-347	3361
	KOL2 replicate 1	105814.1.2	0.67±0.01	-332	3172
	KOL3	105802.1.1	0.94±0.01	-69	504
	KOL4	105800.1.1	0.70±0.01	-302	2820
	KOL3re	105815.1.1	0.65±0.01	-353	3436
	KOL4re	105806.1.1	0.63±0.01	-380	3774
<b>Summer</b>	FPS1	106134.1.1	0.97±0.01	-38	246
	FPS2	106135.1.1	0.96±0.01	-52	365
	Y4	106128.1.1	0.97±0.02	-43	285
	Y3	102311.1.1	0.83±0.01	-177	1499
	Sukharnaya	102304.1.1	0.73±0.01	-274	2503
	Ambolikha	102320.1.1	0.94±0.01	-63	458
	Panteleikha	102305.1.1	0.98±0.01	-24	128
	Filipovkaya	102313.1.1	0.94±0.01	-63	456
	Malenki Annui	102317.1.1	0.66±0.01	-348	3368
	Bolshoi Annui	102318.1.1	0.83±0.01	-175	1477
	KOL1	104321.1.1	0.78±0.02	-231	2040
	KOL1 replicate 1	102314.1.1	0.79±0.01	-213	1855
	KOL1 replicate 2	102315.1.1	0.79±0.01	-208	1806
	KOL2	101944.1.1	0.80±0.01	-205	1781
	KOL2 replicate 1	101945.1.1	0.78±0.01	-222	1953
	KOL2 replicate 2	101946.1.1	0.77±0.01	-239	2131
	KOL3	102301.1.1	0.70±0.01	-306	2869
	KOL4	104322.1.1	0.71±0.01	-296	2748



493 **Table A10.** Sampling date, concentrations of dissolved organic carbon (DOC) and  $\Delta^{14}\text{C}$ -DOC of floodplain stream (FPS), Y4, Y3 and  
 494 Panteleikha sampled during 2006–2011 (previously unpublished data; all sampling by Anya Davydova and Sergei Davydov). The location  
 495 of FPS is N68.73515, E161.40408, thus different from FPS locations in this study. The ETH code is a unique analysis ID assigned for each  
 496 sample analyzed at the Laboratory of Ion Beam Physics, ETH, Zürich.  
 497

Site	Sampling date (dd/mm/yyyy)	DOC ( $\mu\text{M}$ )	ETH code	$\Delta^{14}\text{C}$ (‰)
FPS	06/10/2010	n/a	47880.1.1	57.4
FPS	06/09/2011	613	48172.1.1	69.7
FPS	28/09/2011	483	48165.1.1	71.1
Y4	05/10/2006	1239	48359.1.1	18.2
Y4	15/06/2007	1424	48358.1.1	61.9
Y4	31/07/2007	1837	47879.1.1	23.5
Y4	07/08/2007	2348	47877.1.1	91.2
Y4	16/08/2007	2182	47875.1.1	75.6
Y4	25/09/2007	1825	47874.1.1	62.4
Y4	10/05/2010	n/a	48368.1.1	121
Y4	04/09/2010	n/a	48356.1.1	78.0
Y4	11/09/2010	n/a	47876.1.1	78.7
Y4	04/10/2010	n/a	47878.1.1	56.7
Y4	18/08/2011	1358	48174.1.1	34.2
Y4	06/09/2011	1015	48162.1.1	36.3
Y4	18/09/2011	2116	48164.1.1	81.4
Y4	28/09/2011	1517	48171.1.1	72.4
Y3	05/10/2006	1544	48362.1.1	49.2
Y3	15/06/2007	1550	48357.1.1	64.9
Y3	31/07/2007	2220	47885.1.1	13.7
Y3	07/08/2007	1691	47884.1.1	60.5
Y3	16/08/2007	1717	47883.1.1	55.6
Y3	02/10/2007	n/a	47886.1.1	96.6
Y3	02/10/2007	1719	47881.1.1	80.5
Y3	10/05/2010	n/a	48366.1.1	123
Y3	02/09/2010	n/a	48367.1.1	87.1
Y3	04/09/2010	n/a	48365.1.1	54.5
Y3	18/08/2011	1402	48168.1.1	67.6
Y3	05/09/2011	1310	48163.1.1	63.2
Y3	11/09/2011	n/a	47882.1.1	82.6
Y3	18/09/2011	1620	48173.1.1	81.5
Y3	27/09/2011	1385	48169.1.1	73.6
Panteleikha	18/08/2011	802	48170.1.1	33.3
Panteleikha	06/09/2011	336	48360.1.1	-5.1
Panteleikha	19/09/2011	546	48161.1.1	24.4
Panteleikha	28/09/2011	455	48176.1.1	23.2

498

499

500



501 **Table A11.** Source apportionment results from Markov Chain Monte Carlo analysis showing mean, standard deviation (SD) and quantiles  
 502 (2.5%, 5%, 25%, 75%, 95% and 97.5%) of particulate organic carbon (POC) from active layer, permafrost, autochthonous and terrestrial  
 503 vegetation (terrestrial veg) sources during freshet and summer in floodplain (FPS), headwater, wetland, tundra, forest and Kolyma mainstem.  
 504 For endmembers and further details, see supplementary methods.

	<b>Watershed</b>	<b>Source</b>	<b>Mean</b>	<b>SD</b>	<b>2.50%</b>	<b>5%</b>	<b>25%</b>	<b>50%</b>	<b>75%</b>	<b>95%</b>	<b>97.50%</b>
<b>Freshet</b>	FPS	Active layer	0.085	0.092	0.002	0.003	0.020	0.055	0.118	0.276	0.338
		Permafrost	0.243	0.100	0.054	0.075	0.176	0.245	0.310	0.410	0.445
		Autochthonous	0.632	0.119	0.386	0.431	0.556	0.637	0.712	0.817	0.853
		Terrestrial veg	0.039	0.050	0.000	0.001	0.007	0.021	0.052	0.139	0.173
	Headwater	Active layer	0.150	0.148	0.002	0.004	0.034	0.104	0.227	0.468	0.525
		Permafrost	0.175	0.090	0.031	0.044	0.108	0.168	0.234	0.332	0.365
		Autochthonous	0.597	0.161	0.255	0.316	0.489	0.608	0.717	0.841	0.880
		Terrestrial veg	0.078	0.104	0.000	0.001	0.009	0.034	0.106	0.305	0.377
	Wetland	Active layer	0.061	0.068	0.001	0.002	0.013	0.035	0.086	0.201	0.244
		Permafrost	0.081	0.055	0.009	0.014	0.039	0.069	0.110	0.186	0.211
		Autochthonous	0.821	0.102	0.576	0.625	0.763	0.839	0.897	0.955	0.968
		Terrestrial veg	0.037	0.057	0.000	0.001	0.005	0.015	0.044	0.157	0.203
	Tundra	Active layer	0.327	0.122	0.076	0.117	0.241	0.334	0.413	0.519	0.555
		Permafrost	0.335	0.144	0.092	0.117	0.225	0.324	0.436	0.584	0.634
		Autochthonous	0.095	0.122	0.001	0.001	0.009	0.038	0.138	0.364	0.435
		Terrestrial veg	0.026	0.032	0.001	0.001	0.006	0.015	0.034	0.088	0.116
	Forest	Active layer	0.138	0.113	0.004	0.007	0.047	0.112	0.205	0.359	0.403
		Permafrost	0.269	0.088	0.106	0.126	0.207	0.267	0.328	0.415	0.444
		Autochthonous	0.532	0.110	0.318	0.347	0.456	0.535	0.610	0.709	0.740
		Terrestrial veg	0.061	0.064	0.001	0.002	0.013	0.038	0.088	0.189	0.232
Kolyma	Active layer	0.222	0.181	0.002	0.004	0.052	0.195	0.360	0.544	0.595	
	Permafrost	0.340	0.093	0.148	0.179	0.279	0.346	0.409	0.478	0.502	
	Autochthonous	0.351	0.111	0.152	0.176	0.270	0.345	0.427	0.541	0.574	
	Terrestrial veg	0.087	0.103	0.001	0.001	0.010	0.041	0.137	0.313	0.362	
<b>Summer</b>	FPS	Active layer	0.044	0.052	0.001	0.002	0.010	0.025	0.058	0.151	0.193
		Permafrost	0.116	0.057	0.023	0.034	0.075	0.111	0.152	0.217	0.241
		Autochthonous	0.809	0.090	0.590	0.650	0.763	0.823	0.871	0.926	0.942
		Terrestrial veg	0.031	0.050	0.000	0.001	0.005	0.014	0.035	0.124	0.168
	Headwater	Active layer	0.087	0.101	0.001	0.002	0.015	0.048	0.119	0.298	0.378
		Permafrost	0.088	0.056	0.011	0.017	0.046	0.078	0.119	0.195	0.228
		Autochthonous	0.767	0.137	0.422	0.496	0.694	0.795	0.867	0.942	0.957
		Terrestrial veg	0.058	0.087	0.001	0.001	0.007	0.022	0.067	0.249	0.329
	Wetland	Active layer	0.026	0.032	0.001	0.001	0.006	0.015	0.034	0.088	0.116
		Permafrost	0.034	0.027	0.004	0.005	0.015	0.027	0.047	0.087	0.105
		Autochthonous	0.918	0.058	0.759	0.805	0.895	0.932	0.959	0.981	0.987
		Terrestrial veg	0.021	0.034	0.000	0.001	0.003	0.009	0.025	0.080	0.120
	Tundra	Active layer	0.159	0.149	0.003	0.006	0.038	0.114	0.242	0.456	0.537
		Permafrost	0.215	0.093	0.041	0.064	0.148	0.213	0.278	0.371	0.399
		Autochthonous	0.557	0.141	0.262	0.316	0.463	0.563	0.658	0.782	0.811
		Terrestrial veg	0.070	0.082	0.001	0.002	0.012	0.040	0.098	0.246	0.296
	Forest	Active layer	0.071	0.059	0.004	0.007	0.029	0.055	0.099	0.183	0.222
		Permafrost	0.140	0.056	0.051	0.060	0.099	0.135	0.174	0.239	0.262
		Autochthonous	0.747	0.083	0.559	0.599	0.695	0.757	0.806	0.864	0.880
		Terrestrial veg	0.042	0.042	0.001	0.003	0.012	0.029	0.057	0.128	0.159
Kolyma	Active layer	0.132	0.110	0.003	0.006	0.043	0.105	0.191	0.347	0.405	
	Permafrost	0.216	0.071	0.077	0.098	0.166	0.216	0.264	0.335	0.357	
	Autochthonous	0.589	0.106	0.367	0.403	0.521	0.595	0.664	0.753	0.780	
	Terrestrial veg	0.063	0.067	0.001	0.002	0.013	0.041	0.091	0.198	0.244	

505

506



507 **Data availability**

508 Data will be available within the article or in the Appendix A.

509 **Author contribution**

510 JEV and KHK lead the design of the study with contribution from LB. KHK, LB, DJJ, AD, SD and NZ conducted all the field  
511 work. KHK, LB and DJJ executed all preparatory laboratory work. NH and TIE conducted the AMS analyses, and TT and  
512 PJM analytical laboratory work regarding carbon concentrations and stable isotope analysis. KHK carried out the statistical  
513 analyses. KHK and SBG conducted the spatial analysis. KHK lead the manuscript writing with contribution from all the co-  
514 authors.

515 **Competing interests**

516 The authors declare that they have no conflict of interest.

517 **Acknowledgements**

518 We thank the staff of the Northeast Science Station (NESS) for their support during fieldwork and for providing laboratory  
519 facilities. We want to thank Karel Castro Morales and her team (Friedrich-Schiller University, Jena) and Juri Palmtag  
520 (Northumbria University) for their support in the field. Equally, we want to thank both Suzanne Verdegaal-Warmerdam and  
521 Richard Logtestijn (Vrije Universiteit Amsterdam) for their help with fieldwork preparations. Finally, we thank Niek Speetjens  
522 (Vrije Universiteit Amsterdam) for his advice with the spatial analysis. This study was funded with a starting grant from the  
523 European Research Council to Jorien E. Vonk (THAWSOME #676982), UKRI NERC to Paul J. Mann (CACOON  
524 NE/R012806/1) and NWO Rubicon to Kirsi H. Keskitalo (019.212EN.033). The study of Sergei Davydov, Anna Davydova  
525 and Nikita Zimov was partly carried out within the framework of state assignment number 122020900184-5 of the Pacific  
526 Geographical Institute of RAS.

527 **References**

528 Adams, H. E., Crump, B. C. and Kling, G. W.: Temperature controls on aquatic bacterial production and community dynamics  
529 in arctic lakes and streams, *Environ. Microbiol.*, 12, 1319–1333, doi:10.1111/j.1462-2920.2010.02176.x, 2010.  
530 Battin, T.J., Lauerwald, R., Bernhardt, E.S., Bertuzzo, E., Gómez Gener, L., Hall Jr, R.O., Hotchkiss, E.R., Maavara, T.,  
531 Pavelsky, T.M., Ran, L., Raymond, P., Rosentreter, J.A. and Regnier, P.: River ecosystem metabolism and carbon  
532 biogeochemistry in a changing world, *Nature*, 613, 449-459, doi:10.1038/s41586-022-05500-8, 2023.



- 533 Behnke, M.I., Tank, S.E., McClelland, J.W., Holmes, R.M., Haghypour, N., Eglinton, T.I., Raymond, P.A., Suslova, A.,  
534 Zhulidov, A.V., Gurtovaya, T., Zimov, N., Zimov, S., Mutter, E.A., Amos, E. and Spencer, R.G.M.: Aquatic biomass is a  
535 major source to particulate organic matter export in large Arctic rivers. *Proc Natl Acad Sci*, 120,1–9,  
536 doi:<https://doi.org/10.1073/pnas.2209883120>, 2023.
- 537 Bröder, L., Davydova, A., Davydov, S., Zimov, N., Haghypour, N., Eglinton, T. I. and Vonk, J. E.: Particulate Organic Matter  
538 Dynamics in a Permafrost Headwater Stream and the Kolyma River Mainstem, *J. Geophys. Res. Biogeosciences*, 125, 1–16,  
539 doi:10.1029/2019JG005511, 2020.
- 540 Buchhorn, M., Smets, B., Bertels, L., De Roo, B., Lesiv, M., Tsendbazar, N.-E., Herold, M. and Fritz, S., Copernicus Global  
541 Land Service: Land Cover 100m: collection 3: epoch 2019, Globe 2020, doi: 10.5281/zenodo.3939050, 2020.
- 542 Campeau, A., Wallin, M. B., Giesler, R., Löfgren, S., Mörth, C. M., Schiff, S., Venkiteswaran, J. J. and Bishop, K.: Multiple  
543 sources and sinks of dissolved inorganic carbon across Swedish streams, refocusing the lens of stable C isotopes, *Sci. Rep.*, 7,  
544 1–14, doi:10.1038/s41598-017-09049-9, 2017.
- 545 Collins, C. G., Elmendorf, S. C., Hollister, R. D., Henry, G. H. R., Clark, K., Bjorkman, A. D., Myers-Smith, I. H., Prevéy, J.  
546 S., Ashton, I. W., Assmann, J. J., Alatalo, J. M., Carbognani, M., Chisholm, C., Cooper, E. J., Forrester, C., Jónsdóttir, I. S.,  
547 Klanderud, K., Kopp, C. W., Livensperger, C., Mauritz, M., May, J. L., Molau, U., Oberbauer, S. F., Ogburn, E., Panchen, Z.  
548 A., Petraglia, A., Post, E., Rixen, C., Rodenhizer, H., Schuur, E. A. G., Semenchuk, P., Smith, J. G., Steltzer, H., Totland, Ø.,  
549 Walker, M. D., Welker, J. M. and Suding, K. N.: Experimental warming differentially affects vegetative and reproductive  
550 phenology of tundra plants, *Nat. Commun.*, 12, 1–12, doi:10.1038/s41467-021-23841-2, 2021.
- 551 Dean, J. F., Meisel, O. H., Martyn Rosco, M., Marchesini, L. B., Garnett, M. H., Lenderink, H., van Logtestijn, R., Borges, A.  
552 V., Bouillon, S., Lambert, T., Röckmann, T., Maximov, T., Petrov, R., Karsanaev, S., Aerts, R., van Huissteden, J., Vonk, J.  
553 E. and Dolman, A. J.: East Siberian Arctic inland waters emit mostly contemporary carbon, *Nat. Commun.*, 11, 1–10,  
554 doi:10.1038/s41467-020-15511-6, 2020.
- 555 Denfeld, B. A., Frey, K. E., Sobczak, W. V., Mann, P. J. and Holmes, R. M.: Summer CO<sub>2</sub> evasion from streams and rivers in  
556 the Kolyma River basin, north-east Siberia, *Polar Research* 2013, 32, 19704, doi:10.3402/polar.v32i0.19704, 2013.
- 557 Drake, T. W., Raymond, P. A. and Spencer, R. G. M.: Terrestrial carbon inputs to inland waters: A current synthesis of  
558 estimates and uncertainty, *Limnol. Oceanogr. Lett.*, 3, 132–142, doi:10.1002/lol2.10055, 2018a.
- 559 Drake, T. W., Guillemette, F. and Hemingway, J. D.: The Ephemeral Signature of Permafrost Carbon in an Arctic Fluvial  
560 Network, *J. Geophys. Res. Biogeosciences*, 123, 1475–1485, doi:10.1029/2017JG004311, 2018b.
- 561 Fedorov-Davydov, D. G., Davydov, S. P., Davydova, A. I., Ostroymov, V. E., Kholodov, A. L., Sorokovikov, V. A. and  
562 Shmelev, D. G.: The temperature regime of soils in Northern Yakutia, *Earth’s Cryosph.*, 22, 15–24, doi:10.21782/KZ1560-  
563 7496-2018-4, 2018a.
- 564 Fedorov-Davydov, D. G., Davydov, S. P., Davydova, A. I., Shmelev, D. G., Ostroymov, V. E., Kholodov, A. L. and  
565 Sorokovikov, V. A.: The thermal state of soils in Northern Yakutia, *Earth’s Cryosph.*, 22, 52–66, doi:10.21782/KZ1560-7496-  
566 2018-3, 2018b.



- 567 Guo, L and Macdonald, R.W.: Source and transport of terrigenous organic matter in the upper Yukon River: Evidence from  
568 isotope ( $\delta^{13}\text{C}$ ,  $\Delta^{14}\text{C}$ , and  $\delta^{15}\text{N}$ ) composition of dissolved, colloidal, and particulate phases. *Global Biogeochem. Cycles*, 20,  
569 1-12, doi:10.1029/2005GB002593, 2006.
- 570 Guo, L., Ping, C. L. and Macdonald, R. W.: Mobilization pathways of organic carbon from permafrost to arctic rivers in a  
571 changing climate, *Geophys. Res. Lett.*, 34, 1–5, doi:10.1029/2007GL030689, 2007.
- 572 Harrison, W. G. and Cota, G. F.: Primary production in polar waters: relation to nutrient availability, *Polar Res.*, 10, 87–104,  
573 doi:10.3402/polar.v10i1.6730, 1991.
- 574 Haghipour, N., Ausin, B., Usman, M. O., Ishikawa, N., Wacker, L., Welte, C., Ueda, K. and Eglinton, T. I.: Compound-  
575 Specific Radiocarbon Analysis by Elemental Analyzer-Accelerator Mass Spectrometry: Precision and Limitations *Anal.*  
576 *Chem.*, 91, 2042-2049, doi:10.1021/acsanalchem.8b04491, 2019.
- 577 Holmes, R. M., McClelland, J. W., Peterson, B. J., Tank, S. E., Bulygina, E., Eglinton, T. I., Gordeev, V. V., Gurtovaya, T.  
578 Y., Raymond, P. A., Repeta, D. J., Staples, R., Striegl, R. G., Zhulidov, A. V. and Zimov, S. A.: Seasonal and Annual Fluxes  
579 of Nutrients and Organic Matter from Large Rivers to the Arctic Ocean and Surrounding Seas, *Estuaries and Coasts*, 35, 369–  
580 382, doi:10.1007/s12237-011-9386-6, 2012.
- 581 Hotchkiss, E.R., Hall, R.O., Sponseller, R.A., Butman, D., Klaminder, J., Laudon, H., Rosvall, M. and Karlsson, J.: Sources  
582 of and processes controlling CO<sub>2</sub> emissions change with the size of streams and rivers. *Nat Geosci*, 8, 696-699,  
583 doi:10.1038/ngeo2507, 2015.
- 584 Hotchkiss, E. R., Hall, R. O., Baker, M. A., Rosi-Marshall, E. J. and Tank, J. L.: Modeling priming effects on microbial  
585 consumption of dissolved organic carbon in rivers, *J. Geophys. Res. Biogeosciences*, 119, 982–995,  
586 doi:10.1002/2013JG002599, 2014.
- 587 Hugelius, G., Tarnocai, C., Broll, G., Canadell, J. G., Kuhry, P. and Swanson, D. K.: The northern circumpolar soil carbon  
588 database: Spatially distributed datasets of soil coverage and soil carbon storage in the northern permafrost regions, *Earth Syst.*  
589 *Sci. Data*, 5, 3–13, doi:10.5194/essd-5-3-2013, 2013.
- 590 Keskitalo, K. H., Bröder, L., Jong, D., Zimov, N., Davydova, A., Davydov, S., Tesi, T., Mann, P. J., Haghipour, N., Eglinton,  
591 T. I. and Vonk, J. E.: Seasonal variability in particulate organic carbon degradation in the Kolyma River, Siberia, *Environ.*  
592 *Res. Lett.*, 17, 034007, doi:https://doi.org/10.1088/1748-9326/ac4f8d, 2022.
- 593 Keskitalo, K. H., Bröder, L., Tesi, T., Mann, P. J., Jong, D., Bulte Garcia, S., Zimov, N., Davydova, A., Davydov, S.,  
594 Haghipour, N., Eglinton, T. I. and Vonk, J. E.: PANGAEA data set related to this manuscript. DOI to be added, 2023.
- 595 Levin, I., Kromer, B. and Hammer, S: Atmospheric  $\delta^{14}\text{C}$  trend in Western European background air from 2000 to 2012,  
596 *Tellus, Ser B Chem Phys Meteorol.* 65, 1–7, doi:10.3402/tellusb.v65i0.20092, 2013.
- 597 Mann, P. J., Davydova, A., Zimov, N., Spencer, R. G. M., Davydov, S., Bulygina, E., Zimov, S. and Holmes, R. M.: Controls  
598 on the composition and lability of dissolved organic matter in Siberia’s Kolyma River basin, *J. Geophys. Res. Biogeosciences*,  
599 117, 1–15, doi:10.1029/2011JG001798, 2012.



- 600 Mann, P. J., Eglinton, T. I., McIntyre, C. P., Zimov, N., Davydova, A., Vonk, J. E., Holmes, R. M. and Spencer, R. G. M.:  
601 Utilization of ancient permafrost carbon in headwaters of Arctic fluvial networks, *Nat. Commun.*, 6, 1–7,  
602 doi:10.1038/ncomms8856, 2015.
- 603 Mann, P.J., Strauss, J., Palmtag, J., Dowdy, K., Ogneva, O., Fuchs, M., Bedington, M., Torres, R., Polimene, L., Overduin, P.,  
604 Mollenhauer, G., Grosse, G., Rachold, V., Sobczak W.V., Spencer, R.G.M. and Juhls, B.: Degrading permafrost river  
605 catchments and their impact on Arctic Ocean nearshore processes. *Ambio*, 51, 439-455, doi:10.1007/s13280-021-01666-z,  
606 2022.
- 607 McClelland, J. W., Holmes, R. M., Peterson, B. J., Raymond, P. A., Striegl, R. G., Zhulidov, A. V, Zimov, S. A., Zimov, N.,  
608 Tank, S. E., Spencer, R. G. M., Staples, R., Gurtovaya, T. Y. and Griffin, C. G.: Particulate organic carbon and nitrogen export  
609 from major Arctic rivers, *Global Biogeochem. Cycles*, 30, 629–643, doi:10.1002/ 2015GB005351, 2016.
- 610 Meredith, M., Sommerkorn, M., Cassotta, S., Derksen, C., Ekaykin, A., Hollowed, A., Kofinas, G., Mackintosh, A.,  
611 Melbourne-Thomas, J Muelbert, M. M. C., Ottersen, G., Pritchard, H. and Schuur, E. A. G.: Polar Regions, in IPCC Special  
612 Report on the Ocean and Cryosphere in a Changing Climate, edited by H.-O. Pörtner, D.-O. Pörtner, D. C. Roberts, V. Masson-  
613 Delmotte, P. Zhai, M. Tignor, J. Petzold, B. Rama, and N. M. Weyer., 2019.
- 614 Osburn, C. L. and St-Jean, G.: The use of wet chemical oxidation with high-amplification isotope ratio mass spectrometry  
615 (WCO-IRMS) to measure stable isotope values of dissolved organic carbon in seawater *Limnol. Oceanogr. Methods*, 5, 296-  
616 308, doi:10.4319/lom20075296, 2007.
- 617 Powers, L. C., Brandes, J. A., Miller, W. L. and Stubbins, A.: Using liquid chromatography-isotope ratio mass spectrometry  
618 to measure the  $\delta^{13}\text{C}$  of dissolved inorganic carbon photochemically produced from dissolved organic carbon, *Limnol.*  
619 *Oceanogr. Methods*, 15, 103–115, doi:10.1002/lom3.10146, 2017.
- 620 Rantanen M., Karpechko A.Y., Lipponen A., Nordling, K., Hyvärinen, O., Ruosteenoja, K., Vihma, T., and Laaksonen, A.:  
621 The Arctic has warmed nearly four times faster than the globe since 1979, *Commun Earth Environ*, 3, 1-10,  
622 doi:10.1038/s43247-022-00498-3, 2022.
- 623 Raymond, P.A., Saiers, J.E. and Sobczak, W. V.: Hydrological and biogeochemical controls on watershed dissolved organic  
624 matter transport: Pulse- shunt concept. *Ecology*, 97, 5-16, doi:10.1890/14-1684.1, 2016.
- 625 R Core Team, R: A language and environment for statistical computing. R Foundation for Statistical Computing, Vienna,  
626 Austria. <https://www.R-project.org/>, 2020.
- 627 Santoro, M. & Strozzi, T., Circumpolar digital elevation models > 55° N with links to geotiff images DUEPermafrost\_DEM,  
628 doi:10.1594/PANGAEA.779748, 2012.
- 629 Rogers, J. A., Galy, V., Kellerman, A. M., Chanton, J. P., Zimov, N. and Spencer, R. G. M.: Limited Presence of Permafrost  
630 Dissolved Organic Matter in the Kolyma River, Siberia Revealed by Ramped Oxidation, *J. Geophys. Res. Biogeosciences*,  
631 126, 1–18, doi:10.1029/2020JG005977, 2021.



- 632 Schuur, E. A. G., McGuire, A. D., Schädel, C., Grosse, G., Harden, J. W., Hayes, D. J., Hugelius, G., Koven, C. D., Kuhry,  
633 P., Lawrence, D. M., Natali, S. M., Olefeldt, D., Romanovsky, V. E., Schaefer, K., Turetsky, M. R., Treat, C. C. and Vonk, J.  
634 E.: Climate change and the permafrost carbon feedback, *Nature*, 520, 171–179, doi:10.1038/nature14338, 2015.
- 635 Shiklomanov, A.I., R.M. Holmes, J.W. McClelland, S.E. Tank, and R.G.M. Spencer.: Arctic Great Rivers Observatory.  
636 Discharge Dataset, Version 20211118. <https://www.arcticrivers.org/data>, 2021.
- 637 Siewert, M. B., Hanisch, J., Weiss, N., Kuhry, P., Maximov, T. C. and Hugelius, G.: Comparing carbon storage of Siberian  
638 tundra and taiga permafrost ecosystems at very high spatial resolution, *J. Geophys. Res. Biogeosciences*, 120, 707–723,  
639 doi:10.1002/2015JG002999, 2015.
- 640 Stadnyk, T. A., Tefs A., Broesky, M., Déry, S. J., Myers, P. G., Ridenour, N. A., Koenig, K., Vonderbank, L., Gustafsson, D.;  
641 Changing freshwater contributions to the Arctic: A 90-year trend analysis (1981–2070), *Elementa: Science of the*  
642 *Anthropocene*, 9, 00098, doi:10.1525/elementa.2020.00098, 2021.
- 643 Stock, B.C. and Semmens, B.X.: MixSIAR GUI User Manual, :doi: 10.5281/zenodo.1209993, 2016.
- 644 Stock, B. C. and Semmens, B. X.: Unifying error structures in commonly used biotracer mixing models, *Ecology*, 97, 2562–  
645 2569, doi.org/10.1002/ecy.1517, 2016.
- 646 Strauss, J., Schirrmeister, L., Grosse, G., Fortier, D., Hugelius, G., Knoblauch, C., Romanovsky, V., Schädel, C., Schneider,  
647 T., Deimling, V., Schuur, E. A. G., Shmelev, D., Ulrich, M. and Veremeeva, A.: Deep Yedoma permafrost : A synthesis of  
648 depositional characteristics and carbon vulnerability, *Earth-Science Rev.*, 172, 75–86, doi:10.1016/j.earscirev.2017.07.007,  
649 2017.
- 650 Strauss, J., Laboor, S., Schirrmeister, L., Fedorov, A. N., Fortier, D., Froese, D., Fuchs, M., Günther, F., Grigoriev, M., Harden,  
651 J., Hugelius, G., Jongejans, L. L., Kanevskiy, M., Kholodov, A., Kunitsky, V., Kraev, G., Lozhkin, A., Rivkina, E., Shur, Y.,  
652 Siegert, C., Spektor, V., Streletskaya, I., Ulrich, M., Vartanyan, S., Veremeeva, A., Anthony, K. W., Wetterich, S., Zimov, N.  
653 and Grosse, G.: Circum-Arctic Map of the Yedoma Permafrost Domain, *Front. Earth Sci.*, 9, 1–15,  
654 doi:10.3389/feart.2021.758360, 2021.
- 655 Strauss, J., Laboor, S., Schirrmeister, L., Fedorov, A.N., Fortier, D., Froese, D.G., Fuchs, M., Günther, F., Grigoriev, M.N.,  
656 Harden, J.W., Hugelius, G., Jongejans, L.L., Kanevskiy, M.Z., Kholodov, A.L., Kunitsky, V., Kraev, G., Lozhkin, A.V.,  
657 Rivkina, E., Shur, Y., Siegert, C., Spektor, V., Streletskaya, I., Ulrich, M., Vartanyan, S.L., Veremeeva, A., Walter Anthony,  
658 K.M., Wetterich, S., Zimov, N.S., Grosse, G.; Database of Ice-Rich Yedoma Permafrost Version 2 (IRYP v2). 2022.  
659 doi:<https://doi.org/10.1594/PANGAEA.940078>
- 660 Striegl, R. G., Dornblaser, M. M., Aiken, G. R., Wickland, K. P. and Raymond, P. A.: Carbon export and cycling by the Yukon,  
661 Tanana, and Porcupine rivers, Alaska, 2001-2005, *Water Resour. Res.*, 43, W02144, doi:10.1029/2006WR005201, 2007.
- 662 Tank, S. E., Raymond, P. A., Striegl, R. G., McClelland, J. W., Holmes, R. M., Fiske, G. J. and Peterson, B. J.: A land-to-  
663 ocean perspective on the magnitude, source and implication of DIC flux from major Arctic rivers to the Arctic Ocean, *Global*  
664 *Biogeochem. Cycles*, 26, 1–15, doi:10.1029/2011GB004192, 2012.



- 665 Synal, H. A., Stocker, M. and Suter, M.: MICADAS: A new compact radiocarbon AMS system Nucl. Instr. and Meth. Phys.  
666 Res., 25, 7-13, doi:10.1016/j.nimb.2007.01.138, 2007.
- 667 Turetsky, M. R., Jones, M. C., Walter Anthony, K., Olefeldt, D., Schuur, E. A. G., Koven, C., McGuire, A. D. and Grosse, G.:  
668 Permafrost collapse is accelerating carbon release, Nature, 569, 2019.
- 669 Vonk, J. E., Mann, P. J., Davydov, S., Davydova, A., Spencer, R. G. M., Schade, J., Sobczak, W. V., Zimov, N., Zimov, S.,  
670 Bulygina, E., Eglinton, T. I. and Holmes, R. M.: High biolability of ancient permafrost carbon upon thaw, Geophys. Res. Lett.,  
671 40, 2689–2693, doi:10.1002/grl.50348, 2013.
- 672 Vonk, J. E., Sánchez-García, L., van Dongen, B. E., Alling, V., Kosmach, D., Charkin, A., Semiletov, I. P., Dudarev, O. V.,  
673 Shakhova, N., Roos, P., Eglinton, T. I., Andersson, A. and Gustafsson, Ö.: Activation of old carbon by erosion of coastal and  
674 subsea permafrost in Arctic Siberia, Nature, 489, 137–140, doi:10.1038/nature11392, 2012.
- 675 Waldron, S., Scott, E. M. and Soulsby, C.: Stable isotope analysis reveals lower-order river dissolved inorganic carbon pools  
676 are highly dynamic, Environ. Sci. Technol., 41, 6156–6162, doi:10.1021/es0706089, 2007.
- 677 Walvoord, M. A. and Kurylyk, B. L.: Hydrologic Impacts of Thawing Permafrost – A Review, Vadose Zone Journal, 15, 1–  
678 20, doi:10.2136/vzj2016.01.0010, 2016.
- 679 Welp, L. R., Randerson, J. T., Finlay, J. C., Davydov, S. P., Zimova, G. M., Davydova, A. I. and Zimov, S. A.: A high-  
680 resolution time series of oxygen isotopes from the Kolyma River: Implications for the seasonal dynamics of discharge and  
681 basin-scale water use, Geophys. Res. Lett., 32, 1–5, doi:10.1029/2005GL022857, 2005.
- 682 Wang, L. and Liu, H.: An efficient method for identifying and filling surface depressions in digital elevation models for  
683 hydrologic analysis and modelling. Int. J. Geogr. Inf. Sci., 20, 193-213, doi.org/10.1080/13658810500433453, 2006
- 684 Wild, B., Andersson, A., Bröder, L., Vonk, J., Hugelius, G., McClelland, J. W., Song, W., Raymond, P. A. and Gustafsson,  
685 Ö.: Rivers across the Siberian Arctic unearth the patterns of carbon release from thawing permafrost, Proc. Natl. Acad. Sci. U.  
686 S. A., 116, 10280–10285, doi:10.1073/pnas.1811797116, 2019.
- 687 Winterfeld, M., Goñi, M. A., Just, J., Hefter, J. and Mollenhauer, G.: Characterization of particulate organic matter in the Lena  
688 River delta and adjacent nearshore zone, NE Siberia – Part 2: Lignin-derived phenol compositions, 12, 2261–2283,  
689 doi:10.5194/bg-12-2261-2015, 2015.
- 690 Winterdahl, M., Wallin, M. B., Karlsen, R. H., Laudon, H., Öquist, M. and Lyon, S. W.: Decoupling of carbon dioxide and  
691 dissolved organic carbon in boreal headwater streams, J. Geophys. Res. Biogeosciences, 121, 2630–2651,  
692 doi:10.1002/2016JG003420, 2016.
- 693 Zimov, S. A., Schuur, E. A. G. and Stuart Chapin, F.: Permafrost and the global carbon budget, Science, 312, 1612–1613,  
694 doi:10.1126/science.1128908, 2006.